An N isotopic mass balance of the Eastern Tropical North Pacific Oxygen Deficient Zone

Clara A. Fuchsman[1], Allan H. Devol[1], Karen L. Casciotti[2], Carolyn Buchwald[3,4], Bonnie X. Chang[1,5,6] Rachel E. A. Horak[1]

[1] University of Washington, School of Oceanography, Seattle, WA

[2] Stanford University, Stanford, CA

[3] Massachusetts Institute of Technology/Woods Hole Oceanographic Institution Joint Program in Chemical Oceanography, Woods Hole Oceanographic Institution, Woods Hole, MA

[4] Dalhousie University, Halifax, Nova Scotia, Canada

[5] National Oceanic and Atmospheric Administration, Pacific Marine Environmental Lab, Seattle, WA

[6] JISAO (Joint Institute for the Study of the Atmosphere and Ocean), Seattle, WA

Abstract

Oxygen deficient zones host up to 50% of marine N_2 production and the Eastern Tropical North Pacific (ETNP) is the largest marine oxygen deficient zone. We measured $\delta^{15}N\text{-}NO_3^-$, $\delta^{15}N\text{-}NO_2^-$, and $\delta^{15}N\text{-}N_2$ at 7 stations along a transect normal to the coast in the heart of the ETNP oxygen deficient zone in 2012. The $\delta^{15}N\text{-}N_2$ minimum was 0.34‰ at 300m, which corresponded with the N_2/Ar maximum. When the atmospheric N_2 background was removed, the biological $\delta^{15}N\text{-}N_2$ for the ODZ ranged from -7‰ to -22‰. In the ODZ, $\delta^{15}N\text{-}NO_3^-$ ranged from 15 to 24‰ while $\delta^{15}N\text{-}NO_2^-$ was generally between -11 and -18‰, generating differences up to 40‰ between $\delta^{15}N\text{-}NO_3^-$ and $\delta^{15}N\text{-}NO_2^-$. The isotopic separation between nitrite and nitrogen gas ($\Delta^{15}N_{NO2\text{-}N2}$) changed sign from ~5‰ at the top of the oxygen deficient zone to ~-10‰ at 300m, indicating an important shift in nitrogen cycling with depth. We calculated the closed system Rayleigh isotope effect (ε) for N_2 production from both the $\delta^{15}N$-DIN (ε_{DIN} =26±11‰) and $\delta^{15}N\text{-}N_2$ (ε_{N2}=27±6‰) data. When examined individually by depth, both ε_{DIN} and ε_{N2} matched closely and both ε depth profiles showed maximal fractionation at 300m. Additionally, closed system isotope effects were calculated for one offshore station from the Arabian Sea in 2007 using $\delta^{15}N\text{-}N_2$ (ε_{N2}=24±4‰) and $\delta^{15}N$-DIN (ε_{DIN}=26±3‰). The relatively large isotope effects for N_2 production appear to be found in both major offshore oxygen deficient zones, which implies a large denitrification term in the marine N budget.

KEYWORDS: Nitrogen Isotopes, Oxygen Deficient Zone, Nitrogen Gas, Eastern Tropical North Pacific

1. Introduction

Fixed nitrogen, e.g. nitrate, nitrite and ammonia, is essential for the growth of phytoplankton and other microbes, and limits primary production in much of the surface ocean (Moore et al., 2013). The balance between N_2 fixation and N_2 production controls the amount of marine fixed-N present in the ocean (Brandes and Devol, 2002; DeVries et al., 2012). There are three major oxygen deficient zones (ODZs) in the ocean: the Arabian Sea in the Indian Ocean, the Eastern Tropical North Pacific (ETNP) and the Eastern Tropical South Pacific (ETSP). Despite constituting <1% of the ocean volume, ODZs host 30-50% of marine fixed-N loss through N_2 production (DeVries et al., 2013). Evidence suggests that the oxygen content of the Pacific is decreasing (Ito et al., 2017, 2016; Stramma et al., 2008; Whitney et al., 2007) and a 1% reduction in the ocean O_2 inventory could double the size of ODZs (Deutsch et al., 2011). Indeed, repeat measurements along 110° W longitude in the eastern tropical North Pacific (ETNP) indicate that the ODZ thickness has increased over the past 40 years (Horak et al., 2016). The oxygen content of the ocean is sensitive both to temperature, and to increases in anthropogenic iron deposition (Ito et al., 2016). While the current decrease in oxygen is likely due to anthropogenic impacts and the Pacific Decadal Oscillation, the volume of ODZs should also increase with future climate change (Ito et al., 2016; Ito and Deutsch, 2013). Thus, ODZs are predicted to expand in the future, increasing the area favorable for fixed-N loss.

Although we have a reasonably good idea of the magnitude of fixed-N loss through denitrification (org C + $NO_3^- \rightarrow N_2$) and anammox ($NH_4^+ + NO_2^- \rightarrow N_2$) in the three major ODZs (Chang et al., 2012, 2010), our understanding of the factors affecting these two processes is still limited. The interpretation of the stable isotopic composition of the reactants and products of the N-cycle provides a way to examine low oxygen systems without manipulation or incubation. To date there are relatively few studies examining the $\delta^{15}N\text{-}N_2$ in low oxygen waters (Altabet et al., 2012; Bourbonnais et al., 2015; Brandes et al., 1998; Cline and Kaplan, 1975; Fuchsman et al., 2008; Hu et al., 2016; Manning et al., 2010). Older studies such as Brandes et al (1998) and Cline and Kaplan (1975) examine $\delta^{15}N\text{-}N_2$ in offshore oxygen deficient waters but the authors did not use $\delta^{15}N\text{-}N_2$ to calculate isotope effects. Many of the recent $\delta^{15}N\text{-}N_2$ measurements have been on the Peru shelf of the ETSP and the region offshore of the shelf which is affected by upwelling and eddies (Altabet et al., 2012; Bourbonnais et al., 2015; Hu et al., 2016). In this system, nitrate concentrations are low and can be drawn down to zero. This

differs from far offshore ODZs where nitrate concentrations are consistently between 20 and 30 μM (Chang et al., 2012, 2010). It was found that the isotope effect for N_2 production from nitrate was small, as low as 11‰ on the Peru shelf (Hu et al., 2016) and 14‰ in a eddy off shore of the shelf (Bourbonnais et al., 2015). While no studies in the ETNP and Arabian Seas have previously examined the isotope effect for N_2 production from the N_2 perspective, studies on the isotopic composition of dissolved inorganic N (δ^{15}N-DIN) in offshore oxygen minimum zones in the 1990s has yielded closed isotope effect estimates of ε_{DIN}=22-25‰ (Brandes et al., 1998; Voss et al., 2001). The δ^{15}N-DIN data from the ETNP in 1972 yielded open system isotope effect estimates of 30‰ to 40‰ (Cline and Kaplan, 1975), but the δ^{15}N-DIN values were actually similar to those seen in the 1990s. Thus, current estimates for the N_2 production isotope effect vary from 11‰ to 40‰.

Studies of cultured bacteria also yield large range of estimates for isotope effects involved in steps of N_2 production. Wastewater anammox bacteria have a nitrite reduction isotope effect of ε_{NO2}=16±4‰ (Brunner et al., 2013). Denitrifier cultures grown at slow growth rates and reduced C source produced small isotope effects for nitrate reduction (ε_{NO3}=10 to 15‰; Kritee et al., 2012). However, denitrifier cultures grown at fast growth rates had large isotope effects (ε_{NO3} up to 30‰; (Granger et al., 2008; Kritee et al., 2012). However, the nitrate reduction isotope effect should not be confused with the isotope effect for N_2 production (Fig 1). While Bourbonnais et al (2015) found an isotope effect for N_2 production of 14‰ in an ETSP eddy, they also found an isotope effect for nitrate reduction of 16-21‰. Similarly, a recent modeling study of δ^{15}N-NO_2^- and δ^{15}N-NO_3^- in the ETSP found that an isotope effect of 18-23‰ for nitrate reduction best fit the available data (Peters et al., 2016). This difference between the isotope effect of N_2 production and nitrate reduction highlights the importance of looking at actual δ^{15}N-N_2 data.

In the marine environment, the apparent isotope effect between nitrate and N_2 is affected by nitrite oxidation (Fig 1). Nitrite oxidation has an inverse isotope effect, making nitrite more depleted and nitrate more enriched (Casciotti, 2009). The difference between δ^{15}N-NO_3^- and δ^{15}N-NO_2^- (Δ^{15}N) can reach 40 to 50‰ in low oxygen waters (Bourbonnais et al., 2015; Buchwald et al., 2015; Gaye et al., 2013; Hu et al., 2016; Martin and Casciotti, 2017). Although it has been suggested that ODZs are functionally anoxic (Revsbech et al., 2009; Ulloa et al., 2012), the low oxygen K_m for nitrite oxidation 0.5±4 nM (Bristow et al., 2016), indicates nitrite

oxidation is possible at oxygen concentrations below detection of a STOX oxygen sensor (1-10 nM; Ulloa et al., 2012). Furthermore, rates of oxygen advection and diffusion may be large enough to supply the necessary oxygen to the upper and lower parts of the ODZ, but not the core (Peters et al., 2016). Stable $\delta^{15}N$ and $\delta^{18}O$ isotopes indicate parallel processes of nitrite oxidation and dentrification in ODZs (Buchwald et al., 2015; Gaye et al., 2013; Martin and Casciotti, 2017; Peters et al., 2016). In large ODZs, measured and modeled nitrite oxidation rates dwindle in the core of the ODZ, but the depth range of nitrite oxidation and N_2 production overlap (Babbin et al., 2017, 2014; Buchwald et al., 2015; Peng et al., 2015; Penn et al., 2016; Peters et al., 2016). $\delta^{15}N\text{-}NO_3^-$ and $\delta^{15}N\text{-}NO_2^-$ are affected oppositely by nitrite oxidation, but their combined isotopic pool (DIN) is unaffected. However many N_2 production processes use nitrite directly, so changes in $\delta^{15}N\text{-}NO_2^-$ from nitrite oxidation would affect their N_2 isotopic signature.

Unlike water column denitrification, sedimentary denitrification is thought to usually have a very small isotope effect (<3‰) due to near complete consumption of nitrate (Brandes and Devol, 1997; Lehmann et al., 2007; Sigman et al., 2003). Higher fractionation effects have been documented (Dähnke and Thamdrup, 2013), but in general the isotope effect is thought to be small. The balance between sedimentary denitrification and water column denitrification sets the $\delta^{15}N$ of oceanic DIN. Thus, the isotope effect from nitrate to N_2 during water column denitrification can be used to estimate rates of sedimentary denitrification. A large isotope effect associated with denitrification in offshore ODZs implies significantly more sedimentary denitrification than water column denitrification (Brandes and Devol, 2002). A small fractionation effect for water column denitrification reduces estimates of sedimentary denitrification and requires less N_2 fixation to attain global marine N balance (Altabet, 2007; Bourbonnais et al., 2015; Brandes and Devol, 2002; Kritee et al., 2012). DeVries et al. (2013) were able to model the a balanced ocean N budget with a 3-D biogeochemical model using an apparent isotope effect for nitrate reduction of 17‰ and a marine denitrification rate of 120-240 Tg N yr^{-1} (DeVries et al., 2013). However, an isotope effect significantly larger than 17‰ could potentially imply both larger sources and sinks of N_2 in the ocean.

The Eastern Tropical North Pacific (ETNP) ODZ is the largest Oxygen Minimum Zone (Paulmier and Ruiz-Pino, 2009) with over 700m depth of anoxic water at its heart. Here we present $\delta^{15}N\text{-}N_2$, $\delta^{15}N\text{-}NO_2^-$, and $\delta^{15}N\text{-}NO_3^-$ from 7 stations in the heart of the ETNP ODZ including both coastal and far offshore stations (Figure 2; Table S1). Additionally we examine

135 data from one station in the Arabian Sea (Table S1) to expand the range of our findings. Here we
136 present the first analysis of the denitrification isotopic effect based on $\delta^{15}N\text{-}N_2$ outside of the
137 ETSP.
138
139 **2. Methods**
140 *2.1 Study site and sample collection*
141 Samples were collected during R/V Thomas G. Thompson cruise TN278 to the ETNP
142 during March-April 2012 (Fig. 2, Table S1). Water samples were taken using a SeaBird CTD-
143 Rosette system equipped with dual sensors for conductivity, temperature, and oxygen (SBE 043)
144 as well as Chlorophyll fluorescence and transmissivity. A STOX (Switchable Trace Oxygen
145 microsensor; Revsbech et al., 2009) sensor was also attached to the CTD-Rosette and its output
146 was also logged by the CTD. (The STOX data from this cruise has been previously reported in
147 Tiano et al., 2014). The SeaBird SBE43 oxygen sensor was calibrated against Winkler
148 determinations (n=53 depths in triplicate, regression $R^2 = 0.98$).
149 Samples were also collected on the R/V Roger Revelle at Station 1 (Table S1) in the
150 Arabian Sea during September 2007. Water samples were taken using a SeaBird CTD-Rosette
151 system equipped with dual sensors for conductivity, temperature, and oxygen (SBE 043). The
152 SeaBird SBE43 oxygen sensor was calibrated against micro-Winkler determinations.
153
154 *2.2 Nutrient measurements*
155 For the ETNP, nutrient samples collected directly from the Niskin bottles and were
156 filtered through GF/F glass fiber filters and stored refrigerated until analysis on board.
157 Concentrations of NO_2^-, PO_4^{-3}, $Si(OH)_4$, and NH_4^+ were determined shortly after sample
158 collection using a Technicon Autoanalyzer and the JGOFS protocols (UNESCO, 1994). For the
159 Arabian Sea, nutrient values were reported in Chang et al (2012).
160
161 *2.3 N_2 and $\delta^{15}N\text{-}N_2$ Methods*
162 For the ETNP, duplicate gas samples used for N_2:Ar ratios and $\delta^{15}N\text{-}N_2$ were collected in
163 preweighed, evacuated 185 mL glass flasks sealed with a Louwers-Hapert valve. The sampling
164 flask contained dried mercuric chloride as a preservative (Emerson et al., 1999). To prevent air
165 contamination when sampling, samples were transferred from the Niskin bottle to the sample

166 flask under a local CO_2 atmosphere (Emerson et al., 1999). Sample flasks were filled
167 approximately half full and returned to the University of Washington for analysis. In the
168 laboratory flasks were weighed and equilibrated with the headspace by rotating overnight in a
169 water bath at a known (room) temperature. Immediately after equilibration nearly all liquid water
170 was removed from the flask and the head-space gases were cryogenically processed to
171 completely remove CO_2 and residual water vapor. At the same time a known concentration of
172 ^{36}Ar spike was added to each sample, as done previously (Chang et al., 2010; Fuchsman et al.,
173 2008), to allow the concentration of ^{40}Ar to be determined from the ^{36}Ar:^{40}Ar ratios.
174 To avoid using an oxygen correction for $\delta^{15}N\text{-}N_2$, most oxic samples were also put
175 through an inline CuO furnace to remove all oxygen. However, to check the validity of the
176 oxygen correction, for some duplicates, one sample was put through the furnace and one was not.
177 The still oxygenated samples were measured against an oxygenated standard and an oxygen
178 correction was used as in (Chang et al., 2012, 2010; Fuchsman et al., 2008; Manning et al.,
179 2010). Duplicates matched indicating that present and older data were comparable (Fig. S1). All
180 gas samples were measured at the Stable Isotope Lab, School of Oceanography, University of
181 Washington on a Finnigan Delta XL isotope ratio mass spectrometer. Anoxic samples were
182 measured against a standard containing zero oxygen, where the standard value was determined
183 from air heated in the inline CuO furnace to remove oxygen.
184 Also included here are $\delta^{15}N\text{-}N_2$ measurements from the Arabian Sea in 2007. N_2
185 concentrations for these samples have been previously reported (Chang et al., 2012). However,
186 $\delta^{15}N\text{-}N_2$ values have not been previously reported. They were measured as above except that a
187 CuO furnace was not used. The effect of oxygen on the measurement of $\delta^{15}N$ was determined
188 using a series of five flasks that contain variable amounts of oxygen but the same concentrations
189 and $\delta^{15}N$ of nitrogen gas. The calculated slope from the standards was extrapolated to the
190 sample. The value of the oxygen correction ranged from zero in the ODZ to 0.1 to 0.3‰ in oxic
191 waters.
192 In the Black Sea, a methane correction was used for $\delta^{15}N\text{-}N_2$ (Fuchsman et al., 2008), but in the
193 Black Sea methane reaches 11 µM (Reeburgh et al., 1991). This correction was not needed in the
194 ETNP or Arabian Sea because methane was ≤100 nM in these ODZs (Chronopoulou et al., 2017;
195 Jayakumar et al., 2001).
196

197 *2.4 $\delta^{15}N\text{-}NO_2^-$, and $\delta^{15}N\text{-}NO_3^-$ Methods*

198 Samples containing [NO_2^-] > 0.25 μM were chosen for $\delta^{15}N\text{-}NO_2^-$ analysis, purged with
199 N_2 gas to remove *in situ* N_2O, and treated with a sodium azide/acetic acid reagent (McIlvin and
200 Altabet, 2005). Nitrite isotope analyses were conducted on 2-10 nmol of NO_2^- and calibrated to
201 air and VSMOW reference scales (for $\delta^{15}N$ and $\delta^{18}O$, respectively) using reference materials N-
202 23, N-7373, and N-10219 (Casciotti et al., 2007) each analyzed in triplicate at two different
203 quantities (5 nmol and 10 nmol NO_2^-). $\delta^{15}N\text{-}NO_3^-$ samples were prefiltered with 0.2 μm syringe
204 filters and frozen until returning to the lab. Sulfamic acid was added to samples containing [NO_2^-
205] > 0.2 μM to remove NO_2^- (Granger and Sigman, 2009). $\delta^{15}N\text{-}NO_3^-$ was determined by the
206 'denitrifier method', which involves the bacterial conversion of NO_3^- to N_2O (Casciotti et al.,
207 2002; Sigman et al., 2001). Nitrate isotope analyses were conducted on 20 nmol NO_3^- and
208 calibrated to air and VSMOW reference scales (for $\delta^{15}N$ and $\delta^{18}O$, respectively) using reference
209 materials USGS32, USGS34, and USGS35 (Bohlke et al., 2003), each analyzed six times
210 throughout the run in 20 nmol amounts (McIlvin and Casciotti, 2011). $\delta^{15}N\text{-}NO_2^-$, and $\delta^{15}N\text{-}NO_3^-$
211 from station 1 in the Arabian Sea 2007 were measured similarly and can be seen in Martin and
212 Casciotti (2017).
213
214 **3. Results**

215 The section comprised by our stations in the ETNP showed a significant upward tilt of
216 the isopleths surfaces near the coast (Fig. 3). At stations 132 and 133, the stations closest to the
217 coast (Fig. 2), the top of the ODZ and the nitrite maximum were at shallower depths than open
218 ocean stations on the transect (Fig. 3). Due to this we present the offshore stations data versus
219 depth, but when all stations are combined we plot versus density. At the offshore stations (Fig. 2)
220 the STOX based O_2 concentrations became undetectable at 105 m and remained undetectable
221 until 830 m (Tiano et al, 2014). We define the ODZ as this zone over which oxygen was below
222 detection.

223 The top of the ODZ was also the depth at which a secondary nitrite maximum (SNM)
224 appeared in the water column (Fig. 2a). At the offshore stations, the concentration of NO_2^- in the
225 SNM increased to ~5 μM at 140 m and then decreased to zero at 500m (Fig. 2a), while at the
226 coastal stations the maximum was greater (~6 μM) and occurred shallower in the water column
227 (Fig. 3 and S2). Nitrate concentrations were very low in the mixed layer, increased rapidly in the

pycnocline to about 20 μM, then increased more gradually to a maximum of about 45 μM at 1000 m (Fig. 3a). Ammonium concentrations were generally <0.1 μM in the ODZ (Peng et al., 2015; Figure S3), so we consider DIN to be NO_3^- + NO_2^-. DIN concentrations were similar to nitrate with the exception of a significant elevation in the upper half of the ODZ due to the secondary nitrite maximum.

Data from all stations, coastal and offshore, aligned well on density surfaces (Fig. S4). At all stations, the SNM peak was located on the 26.2 sigma-theta surface. This sigma-theta surface coincides with the Pacific Equatorial 13ºC water mass (Fig. S5) discussed in (Fiedler and Talley, 2006).

3.1 Nitrogen Gas and $\delta^{15}N$

Measured N_2:Ar saturation ratios were high in the ODZ and frequently had two local maxima, one at the top of the ODZ and a second at 300m (Fig. S2). Measured N_2:Ar ratios contain both biologically produced N_2 and a large background signal. The background N_2 (and argon) was originally derived from equilibrium with air, but mixing of water masses of different temperatures causes gases to become supersaturated in the ocean (Ito and Deutsch, 2006). We determined biological N_2 (N_2 excess) by subtracting background N_2:Ar measurements from oxic waters in the tropical and subtropical Pacific (Chang et al., 2012). The background data was fit with the equation:

$$N_2{:}\,Ar_{Background} = 0.998 + 2.31 \times 10^{-8} e^{0.49\sigma_\theta} \text{ (Chang et al., 2012).} \quad (1)$$

Calculated background values for each station are shown in Fig. S2. N_2 excess, which we consider to be biological N_2, was then calculated as follows:

$$N_{2,excess} = (N_2{:}\,Ar_{measured} - N_2{:}\,Ar_{Background}) \times N_{2,saturation} \times 2 \quad (2)$$

Where the factor of 2 in the last term converts from moles of N_2 gas to moles N. $N_{2,saturation}$ was calculated as in Hamme and Emerson (Hamme and Emerson, 2004). Thus Ar measurements were not used in the calculation of N_2 excess reported here. Argon concentrations were up to 6% supersaturated in the upper oxic waters, but were very close to saturation in the

ODZ (Fig S6). Since the argon measurements were close to saturation, using Ar measurements to determine N_2 concentrations from N_2/Ar measurements and background calculations, instead of $N_{2,saturation}$, produced quite similar results (Fig. S7). N_2 excess values were high through the ODZ with concentrations between 10 and 15 μM (Fig. 4 and S2).

The amount of fixed N loss in an ODZ, has frequently been expressed as N deficit, which is the difference between measured [DIN] and expected DIN. The expected DIN ($N_{expected}$) is typically estimated from phosphate to DIN ratios determined from waters outside the ODZ and phosphate concentrations within the ODZ:

$$N_{expected,ETNP} = 14.4 \times [PO_4^{3-}] - 1.1 \quad \text{(Chang et al., 2012).} \qquad (3)$$

In the ETNP, depth distribution of N deficit generally matches N_2 excess (Fig. 4), with N deficit, like N_2 excess, maximal at the top of the ODZ and at 300m. There is a local minimum in both N deficit and N_2 excess located at 200 m (density surface 26.3). In general, N_2 excess and N deficit values match closely with a slope of 0.9 (R^2=0.86; Fig. S8). However, at stations 162 and 163 there is a significant mismatch (2-4 μM) between N deficit and N_2 excess in the ODZ (Fig. S2). The reasons for this mismatch are unknown, but are likely related to our background values imperfectly capturing the actual background due to water mass mixing.

The ETNP $\delta^{15}N$-N_2 measurements range from 0.34 to 0.62‰ and frequently have a minimum <0.4‰ at 300m (Fig. S2). These measurements are similar to $\delta^{15}N$-N_2 data from the ETNP in 1993 (Brandes et al., 1998). Measured $\delta^{15}N$-N_2 also contains both a biological and background signals. The $\delta^{15}N$-N_2 value in seawater at equilibrium with air is about 0.68±0.02‰ (Knox et al., 1992). Mixing has a much smaller effect on $\delta^{15}N$ isotopes than on N_2 concentrations since all water masses bear the equilibrium isotope signature. The average $\delta^{15}N$-N_2 measurements at 1500m, a depth not influenced by the ODZ, at the 4 offshore stations (data not shown) was 0.65±0.05‰. Here we used 0.68‰ as our background value, but also made calculations using values of 0.65‰ and 0.7‰ in order to estimate potential error in the calculation of $\delta^{15}N$-N_2 excess (Fig. S2). The resulting $\delta^{15}N$-N_2 excess values for the ETNP were generally between -10‰ and -30‰ (Fig. 4 and S2, S4).

Total $\delta^{15}N\text{-}N_2$ for the Arabian Sea ranged from 0.45‰ to 0.55‰ (Fig. S9). Despite this, $\delta^{15}N\text{-}N_2$ excess values for the Arabian Sea, calculated as above but using $N_2{:}Ar_{background}$ calculations from the Arabian Sea (Chang et al., 2012) were between -14‰ and -20‰ (Fig. 5), which is in the same range as the ETNP.

In the ETNP, the $\delta^{15}N\text{-}NO_3^-$ increased from around 10‰ in the oxycline to around 20‰ in the ODZ and then values decreased towards the lower oxycline (Fig. 4). In the Arabian Sea, $\delta^{15}N\text{-}NO_3$- was 11-12‰ at the top and bottom of the ODZ, but reached 24‰ in the heart of the ODZ (Fig. S10). The ETNP $\delta^{15}N\text{-}NO_2$- was generally in the -15‰ to -20‰ range in the ODZ (Fig. 4 and S2). While $\delta^{15}N\text{-}NO_2^-$ had similar range of values as $\delta^{15}N\text{-}N_2$ excess, at each station $\delta^{15}N\text{-}N_2$ excess was enriched compared to $\delta^{15}N\text{-}NO_2^-$ in the upper ODZ, but became more depleted than $\delta^{15}N\text{-}NO_2^-$ at 200-300m (Fig. S2). In the Arabian Sea, $\delta^{15}N\text{-}NO_2$- and $\delta^{15}N\text{-}N_2$ excess were quite similar at ~-15‰ until 250 m, where $\delta^{15}N\text{-}NO_2$- started to become more depleted with depth reaching -31‰ at 375m (Fig 5). $\delta^{15}N\text{-}NO_2^-$ values from the Arabian Sea ODZ (Fig 5) are similar to those seen in the ETNP in 2012.

In the ETNP, nitrite concentrations were 5 µM offshore and reached 6 µM closer to the coast (Fig. 3) which is unusually high for the ETNP (Horak et al., 2016). Accordingly, $\delta^{15}N\text{-}NO_2^-$ was different in 2012 than values seen in the ETNP in 2003 (Casciotti and McIlvin, 2007). In 2003, $\delta^{15}N\text{-}NO_2^-$ values changed from -15‰ to -18‰ at the top of the ODZ to -8‰ at 300m (Casciotti and McIlvin, 2007). In contrast, in 2012 the $\delta^{15}N\text{-}NO_2^-$ values were more negative at depth than in 2003, with values at 300m of -12‰ to -15‰ (Fig. 4, S2). We suspect that this is due to the higher nitrite concentrations in 2012 than seen in 2003 (3.5 µM). It is still unclear why these differences occurred (Horak et al., 2016), but larger concentrations should buffer the enrichment of the remaining nitrite as it is reduced.

3.2 $\Delta^{15}N$ values

A comparison between different N species $\delta^{15}N$ values helps quantify the importance of oxidation and reduction in the system (Casciotti, 2009; Casciotti et al., 2013). $\Delta^{15}N_{NO3\text{-}NO2}$, the difference between $\delta^{15}N\text{-}NO_3^-$ and $\delta^{15}N\text{-}NO_2^-$, was consistently about 32‰ through most of the ETNP ODZ, though values may be slightly smaller below 300m (Fig. 6). Similar results were found in 2003 ETNP data (Casciotti and McIlvin, 2007). In the Arabian Sea, the $\Delta^{15}N_{NO3\text{-}NO2}$

was ~35‰ at the top of the ODZ but was ~40‰ for the majority of the ODZ (Fig. S9). Interestingly, the $\Delta^{15}N_{NO3\text{-}NO2}$ had significantly more structure in the ETSP (Casciotti et al., 2013) than seen here in the ETNP and Arabian Seas. The $\Delta^{15}N_{NO3\text{-}NO2}$ values seen here are greater than ~25‰, an upper estimate on the isotope effect (ε) value for nitrate reduction (Granger et al., 2008), indicating the influence of nitrite oxidation on the system (Casciotti et al., 2013). Nitrite oxidation has an inverse fractionation effect, which means that the nitrate produced becomes more enriched and the nitrite remaining becomes more depleted (Buchwald and Casciotti, 2010; Casciotti, 2009). Thus, nitrite oxidation can increase the isotopic separation between NO_3^- and NO_2^-. The more nitrite oxidation the greater the $\Delta^{15}N_{NO3\text{-}NO2}$ (Casciotti et al., 2013). However, one would expect that nitrite oxidation to be higher at the edges of the ODZ (Babbin et al., 2017; Penn et al., 2016; Peters et al., 2016), and $\Delta^{15}N_{NO3\text{-}NO2}$ does not follow this trend both for the ETNP and the Arabian Sea (Fig 6, S10). We also looked at $\Delta^{15}N_{N2\text{-}NO2}$, the $\delta^{15}N$ difference between excess N_2 and nitrite for the ETNP. These values consistently become more depleted with depth, changing sign from 2‰ to10‰ at the top of the ODZ to –6‰ to -15‰ at 300m (Fig. 6). $\Delta^{15}N_{N2\text{-}NO2}$ values highlight that $\delta^{15}N\text{-}N_2$ excess was enriched compared to $\delta^{15}N\text{-}NO_2^-$ in the upper ODZ, but became more depleted than $\delta^{15}N\text{-}NO_2^-$ at 200-300m (Fig. 6, S2). The change between positive to negative $\Delta^{15}N_{N2\text{-}NO2}$ occurs at the nitrite maximum, which is in the 13°C water mass. Interestingly, the positive $\Delta^{15}N_{NO2\text{-}N2}$ in the top 50m of the ODZ indicates that the N_2 produced is more enriched than nitrite even though nitrite is the source of N_2 (Fig. 6). Isotope effects for nitrite reduction of ε=22‰ have been found in bacterial cultures containing the copper-type nitrite reductase (NirK) and ε=8‰ in cultures containing the heme-type nitrite reductase (NirS) (Martin and Casciotti, 2016). In an eddy in the ETSP, the isotope effect for nitrite reduction was calculated to be 12‰ (Bourbonnais et al., 2015), similar to cultures with the NirK copper nitrite reductase (Martin and Casciotti, 2016). However, *in situ* nitrite data has been successfully modeled with no fractionation during nitrite reduction in the Southern ETNP (Buchwald et al., 2015) and ETSP (Casciotti et al., 2013; Peters et al., 2016), and $\delta^{15}N\text{-}NO_2^-$ and $\delta^{15}N\text{-}N_2$ excess values were nearly identical in the Arabian Sea (Fig 5). Scenarios to explain this data are discussed below (section 4.3).

3.3 Isotope effect for N_2 production

To minimize the complication of nitrite oxidation on our calculations, we combine δ^{15}N-NO_2^-, and δ^{15}N-NO_3^- to form δ^{15}N-DIN. We calculated the closed system fractionation effect for N_2 production from δ^{15}N-DIN and from δ^{15}N of biologically produced N_2 (δ^{15}N-N_2 excess). Closed system calculations assume no re-supply of substrate, in this case nitrate, so are appropriate where there is little mixing (Hu et al., 2016). As our stations were far removed from the edges of the ODZ where mixing and re-supply of nitrate would occur, we chose a closed system isotope effect calculation. Individual isotope effects were calculated for each sample using the equations for closed system fractionation (Mariotti et al., 1981):

$$\delta^{15}DIN = \delta^{15}DIN_{initial} + \varepsilon \times \ln[f] \quad (4)$$

$$\delta^{15}N_{2,excess} = \delta^{15}DIN_{initial} - \varepsilon\left(\frac{f}{1-f}\right)\ln[f] \quad (5)$$

where ε is the isotope effect and f is the fraction of DIN remaining. In all cases, values for f were calculated as:

$$f = \frac{NO_3^- + NO_2^-}{DIN_{expected}} \quad (6)$$

where

$$DIN_{expected} = NO_3^- + NO_2^- + N_{2,excess} \quad (7)$$

Thus, instead of calculating expected DIN based on an assumed N:P ratio, $N_{2,excess}$ measurements were used to quantify the amount of DIN removed. The isotope effect for nitrate reduction was calculated similarly to DIN. Also, instead of assuming a deep water value for δ^{15}N-$DIN_{initial}$, we calculated δ^{15}N-$DIN_{initial}$ by combining the mass-weighted isotopes of nitrate, nitrite, and N_2 excess (Figure S11) which contains the influence of remineralized organic matter as well as the original nitrate. In the ODZ, we assumed that remineralized organic matter is converted to N_2 via anammox. For this calculation, we assumed that N_2 fixation rates were negligible. Offshore nitrogen fixation rates measured in the ODZ on this cruise were 0.2 nM per day (Jayakumar et al., 2017), supporting this assumption. We did not include N_2O in this calculation, but N_2O concentrations were from 0-60 nM in the ODZ for this cruise (Babbin et al., 2015), so were insignificant to the calculation when mass-weighted. Ammonium concentrations were also generally below detection in the ODZ (Peng et al., 2015). Averaging across all samples yielded δ^{15}N-$DIN_{initial}$ of 5.3 ± 0.8‰ for the ETNP and 5.6‰ ± 0.9‰ for the Arabian Sea. These average values were used as δ^{15}N-$DIN_{initial}$ in our calculations. Our average δ^{15}N-$DIN_{initial}$ values of 5.3‰ and 5.6‰ are very similar to those used in previous isotope effect calculations in the

ETSP (5.5‰; Bourbonnais et al., 2015; Hu et al., 2016). However, more enriched $\delta^{15}N\text{-}NO_3^-$ values have been found for the intermediate waters at station ALOHA (6.4‰; Sigman et al., 2009) and in the 200-600m Pacific equatorial waters (7‰; Rafter et al., 2013). Thus $\delta^{15}N\text{-}DIN_{initial}$ in the ODZ is more depleted than nitrate in the ODZ source waters. By using this calculated $\delta^{15}N\text{-}DIN_{initial}$ based on our data, we avoid the over estimation of the N_2 production isotope effect due to aerobic respiration as discussed by Marconi et al (2017). If $\delta^{15}N\text{-}DIN_{initial}$ were chosen from source waters, the addition of remineralized organic N would be incidentally included in the isotope effect calculation (Marconi et al., 2017). In fact, given the relatively enriched source waters, it does appear that our depleted $\delta^{15}N\text{-}DIN_{initial}$ values are probably due to the influence of remineralization. Sediment trap samples from our ETNP cruise had a $\delta^{15}N$ of 8.1±0.4‰ offshore (n=2) and 8.7±0.4‰ onshore (n=5) (Table S2; Rick Keil, personal communication). Due to little seasonality in the chlorophyll a, productivity, and nitrate supply in our region of the ETNP (Pennington et al., 2006), we assume that the isotopic composition of our sediment trap samples were representative. Sediment trap material from the Arabian Sea 2007 ODZ (collection described in Keil et al., 2016) had $\delta^{15}N$ of 7±1‰ (n=12; Table S2; Rick Keil, personal communication), similar to values from the ETNP. Given a isotope effect for organic matter remineralization to ammonium of 4‰ (Macko et al., 1994; Saino and Hattori, 1980; Wada, 1980), remineralized N should have been ~4 to 5‰ in the ODZ, similar to our $\delta^{15}N\text{-}DIN_{initial}$ of 5.3 ± 0.8‰ or 5.6‰ ± 0.9‰.

When calculated for each depth, the closed isotope effects for the ETNP derived from DIN and N_2 excess match closely; they are -20 to -25‰ at the top of the ODZ, increase to -30 to -45‰ at ~300m, and then decrease again toward the bottom of the ODZ (Fig. 7, and S12). In the Arabian Sea, the closed isotope effects derived from DIN and N_2 excess were fairly constant, varying between -24‰ and -30‰ (Fig 8). As expected, in both the ETNP and the Arabian Sea, $\delta^{15}N\text{-}NO_2^-$ was often most depleted at the top of the ODZ, where one would expect nitrite oxidation (Fig. 5, and S2). However, unlike the Arabian Sea, where $\delta^{15}N\text{-}NO_2^-$ and $\delta^{15}N\text{-}N_2$ are closely correlated for the top 300m and $\delta^{15}N\text{-}N_2$ is fairly constant with depth (Fig 5), in the ETNP, $\delta^{15}N\text{-}N_2$ excess does not track $\delta^{15}N\text{-}NO_2^-$, and $\delta^{15}N\text{-}N_2$ excess has the most depleted values in 250m-300m range towards the bottom of the SNM (Fig. 4, S2, S4). Unsurprisingly, 250m-300m is the same range where the isotope effects are the largest (Fig. 7, Fig S12).

For the ETNP, the average apparent closed isotope effect for consumption of DIN was -26±11‰ (using equation 4) and it was -27±6‰ for production of N_2 excess (using equation 5). The closed isotope effect from St 132, our ETNP coastal station (-23±3‰ for N_2 and -23±5‰ for DIN; 550 m bottom depth; Fig. 7), is similar to our offshore average value (-29±5‰ for N_2). If the closed isotope effect for the ETNP was calculated by the more traditional Rayleigh plot, the values were quite similar to our average depth calculations (-25.1‰ for DIN; Figure S13), but due to the previously mentioned variability with depth, the R^2 value was only 0.5 for DIN and was worse for N_2 gas (data not shown). Though we prefer a closed system calculation, we also examined our results with an open system calculation where mixing is assumed to be a dominant process:

$$\delta^{15}DIN = \delta^{15}DIN_{initial} + \varepsilon \times (1 - f) \quad (8)$$

$$\delta^{15}N_{2,excess} = \delta^{15}DIN_{initial} - \varepsilon \times f \quad (9).$$

Our isotope effects were similar, though more variable, if an open system calculation was used (-29±17‰ for DIN and -32±8‰ for N_2 in the ETNP). This similarity between closed and open systems supports the robustness of our calculations. Given that the N deficit (calculated from nutrients) and the N_2 excess (calculated from N_2 gas) were quite similar (Fig. 4, S2, S4, S8), as were the isotope effects calculated from reactants and from the product, we assume that we have mass balance in our system.

The Arabian Sea is another major ODZ. We have δ^{15}N-N_2 excess and δ^{15}N-DIN from one offshore station from Arabian Sea in 2007 (R/V Revelle) (Fig. 5). Sediment trap material from the Arabian Sea 2007 ODZ (Keil et al., 2016) had δ^{15}N of 7±1‰ (n=12; Table S2; Rick Keil, personal communication), similar to values from the ETNP. Thus it is not surprising that δ^{15}N-$DIN_{initial}$ was also similar (5.6‰ ± 0.9‰). When δ^{15}N-N_2 is examined from the Arabian Sea, the closed isotope effect was 26±4‰ and the isotope effect for δ^{15}N-DIN was 26±3‰ (Fig. 8), which is also similar to the offshore ETNP. These numbers are significantly larger than those determined from the coastal ETSP data (Hu et al., 2016) but are consistent with older δ^{15}N-DIN data from the Arabian Sea in 1993, 1994, and 1995 (ε=22±3‰ with a δ^{15}N-$DIN_{initial}$ of 6‰ and ε=24 with δ^{15}N-$DIN_{initial}$ of 5‰) and ETNP in 1993 (ε=25±2‰ with a δ^{15}N-$DIN_{initial}$ of 6‰) and in the ETNP in 1997 (ε=22.5‰ with a δ^{15}N-$DIN_{initial}$ of 6.2‰) (Brandes et al., 1998; Voss et al., 2001). Combined, this data indicates that the isotope effect for N_2 production is similar for the offshore regions of these two ODZs and is approximately 25‰.

The isotope effect for nitrate reduction in the ETNP was -28±6‰, which was in the same range as the isotope effect for DIN. In Arabian Sea the isotope effect for nitrate reduction was -25±6‰, also in the same range as the isotope effect for DIN. This differs from the ETSP where isotope effect for nitrate reduction has been repeatedly found to be significantly larger than that for DIN conversion to N_2 (Bourbonnais et al., 2015; Casciotti et al., 2013; Peters et al. this issue).

4. Discussion

The Eastern Tropical North Pacific (ETNP) ODZ is the largest marine ODZ by volume and accounts for ~40% of marine anoxic waters by area (Paulmier and Ruiz-Pino, 2009). At offshore stations in the core of the ODZ in 2012, oxygen was below detection for a STOX sensor from 105 m to 800 m. Both rates of N_2 production by denitrification and anammox were measured in incubation experiments during this cruise (Babbin et al., 2015, 2014) and the addition of sediment trap material stimulated denitrification rates (Babbin et al., 2014). Denitrifier RNA has been found to be enriched within particles in the ETNP (Ganesh et al., 2015). The Arabian Sea only accounts for 8% of marine anoxic waters by area, but thickness of the ODZ is comparable to the ETNP (Paulmier and Ruiz-Pino, 2009). On our cruise in the Arabian Sea in 2007, denitrification rates and genes dominated over anammox (Ward et al., 2009) and the addition of sediment trap material stimulated denitrification rates (Chang et al., 2014). N_2 gas and $\delta^{15}N$, $\delta^{15}N\text{-}NO_2^-$ and $\delta^{15}N\text{-}NO_3^-$ were measured along a coast to open ocean transect in core of the ETNP ODZ and on one station in the Arabian Sea. Interestingly in the ETNP, $\Delta^{15}N_{NO2\text{-}N2}$ changed with a clear trend from negative to positive with depth and the isotope effects for N_2 production also changed with depth. These same features were not seen in the Arabian Sea. In both the ETNP and Arabian Sea, the isotope effects calculated from DIN and N_2 were quite similar, and the magnitude of the isotope effect was large.

4.3 Change in isotope effect with depth

In the ETNP, the absolute values of the apparent isotope effects for DIN and N_2 excess increase with depth until ~300m and then decrease again (Fig. 7, S12). This same change in isotope effects with depth is not seen in the Arabian Sea (Fig 8). Instead in the Arabian Sea there is a slight decrease in apparent isotope effect with depth (Fig 8). Below we discuss 6 possible explanations for this observation in the ETNP. One hypothesis to explain this could be the

influence of nitrite oxidation at the top of the ODZ. $\delta^{15}N\text{-}NO_3^-$ and $\delta^{15}N\text{-}NO_2^-$ values from the Southern ETNP (Costa Rica Dome) were similar to values presented here and could be modeled completely by nitrate and nitrite reduction, with nitrite oxidation (Buchwald et al., 2015) but N_2 gas was not included in the model. Nitrite oxidation could affect the system by modifying $\delta^{15}N\text{-}NO_2^-$, and $\delta^{15}N\text{-}NO_3^-$ and by affecting the nitrite concentrations. Isotope effects are often reduced at low substrate concentrations. However, the DIN and N_2 excess isotope effects are largest at 250-300m where nitrite concentrations are already greatly reduced, so nitrite concentrations cannot explain the isotope effect depth profile. Additionally, nitrite oxidation would affect the intermediate reactant $\delta^{15}N\text{-}NO_2$-, which could then affect $\delta^{15}N\text{-}N_2$ and the isotope effect. However, $\delta^{15}N\text{-}NO_2$- and $\delta^{15}N\text{-}N_2$ excess do not correlate in the 250-300m region, implying a different cause for the change in isotope effect. All together, nitrite oxidation does not appear to be responsible for the change in isotope effects with depth.

A second hypothesis would involve the input of ammonium into the ODZ from migrating micronekton/zooplankton. ADCP data indicates micronekton migrate to 300m in the ETNP (Bianchi et al., 2014). $\delta^{15}N$ of ammonium from excretion under ODZ conditions is not well quantified. Theoretically, the input of depleted ammonium from zooplankton at 300m could affect $\delta^{15}N\text{-}N_2$ gas, making it more depleted. However, any significant depletion from injected ammonium would also appear in our $DIN_{initial}$ calculations, and it does not (Figure S11).

A third hypothesis is that the differences in isotope effects are due to differences in physical processes. The T/S diagram (Fig. S5), shows that the nitrite maximum is in the Pacific Equatorial 13ºC water (Fiedler and Talley, 2006). The anoxic water masses above and below could carry different signals that would then mix. Theoretically, the calculated DIN fractionation effect in the 13ºC water could be affected by mixing with oxic water above it (Marconi et al., 2017). In fact, the enriched $\delta^{15}N\text{-}NO_3^-$ in the oxycline above the ODZ (Fig. 4) suggests that mixing is occurring. However, calculation errors from this mixing would be, once again, related to incorrect choice of $\delta^{15}N\text{-}DIN_{initial}$. Since our $\delta^{15}N\text{-}DIN_{initial}$ (section 4.2) and $DIN_{expected}$ (Eq 7) are calculated from our DIN and N_2 data without assumptions that could vary with water mass, it remains unclear why the different water masses would have different fractionation effects.

Because the $\Delta^{15}N_{NO3\text{-}NO2}$ has little variability from the top of the ODZ to 300m while $\Delta^{15}N_{NO2\text{-}N2}$ changes with a clear trend (Fig. 6), it seems possible that the change in isotope effect for N_2 production with depth has to do with nitrite reduction. A fourth hypothesis to explain the

difference in isotope effects with depth would be a change in the N_2 producing bacterial community at 200-400m. Different types of bacteria are known to have different nitrite reduction isotope effects based on their type of nitrite reductase (Martin and Casciotti, 2016). However, *nirK* was the dominant nitrite reductase gene throughout the ODZ (Fuchsman et al., 2017) and $\Delta^{15}N_{NO2\text{-}N2}$ values were positive in the upper ODZ and negative below, switching sign at the nitrite maximum. It seems unlikely that some bacteria would have a positive isotope effect for nitrite reduction and other bacteria would have a negative nitrite reduction isotope effect. However, it is possible that some denitrifiers could use nitrate as an oxidant, and keep and use the nitrite produced internally, while others use nitrite from the bulk water column. Given the large difference in $\delta^{15}N$ between nitrate and nitrite, these two hypothetical types of bacteria would produce very different $\delta^{15}N\text{-}N_2$. For example, at 100m a denitrifying bacterium using nitrate would start with a reactant at ~12‰ while a bacterium using nitrite would start with a reactant at ~ -18‰. For the nitrate case, an isotope effect of ~20‰ would explain the $\delta^{15}N\text{-}N_2$ excess (-12 to -18‰) at 100m while the nitrite case would need a reverse isotope effect. However, at 300m, nitrate is 20‰ while nitrite is -14 to -16‰. Thus a nitrite reduction isotope effect of 10‰ would successfully explain $\delta^{15}N\text{-}N_2$ excess (~-26‰) at 300m while an isotope effect from nitrate would be exceptionally large (46‰). It appears that a switch in the type of denitrifier could reproduce our measurements. What is unclear is if these two types of bacteria actually exist. In gram negative bacteria, nitrite reduction occurs in the periplasm (Zumft, 1997), where nitrite can escape the cell across the outer membrane. However, an internal nitrite pool has been demonstrated for denitrifying bacteria in a sulfidic fjord (Jensen et al., 2009). The idea is that if a bacterium performs both nitrate reduction and nitrite reduction, some nitrite may escape the cell, but the nitrite concentrations inside the cell is still higher than its surroundings (Jensen et al., 2009). Additionally, the use of an internal nitrite pool for at least some denitrifiers has been suggested previously in the ETSP and Arabian Seas to explain excess $\delta^{29}N_2$ produced in enriched ^{15}N experiments with nitrite (Chang et al., 2014; De Brabandere et al., 2014).

Additionally the apparent isotope effects for nitrate and nitrite reduction could be reduced at the top of the ODZ due to assimilation. Cyanobacteria are photosynthesizing at the top of the ODZ in the ETNP (Garcia-Robledo et al., 2017), so are presumably assimilating nitrogen in some form. Assimilation has a small isotope effect of 5-7‰ (Altabet, 2001; Granger et al., 2004)

and so could be reducing the combined apparent isotope effect at the top of the ODZ. However, neither assimilation of nitrate nor of nitrite can explain the $\Delta^{15}N_{NO2\text{-}N2}$ changes in sign.

Finally, denitrifiers are known to be attached to particles (Ganesh et al., 2015, 2014). Given sediment trap data ($\delta^{15}N$ of organic N of 8‰), in the ETNP, and with a isotope effect for organic matter remineralization to ammonium of 4‰ (Macko et al., 1994; Saino and Hattori, 1980; Wada, 1980), nitrite produced from remineralized ammonium within particles would be enriched compared to the highly depleted, water column nitrite measurements. Low levels of particle associated nitrite has been found in oxic waters at Station ALOHA (Wilson et al., 2014). The presence of nitrite has been showed to stimulate N_2O production in particles at Station ALOHA (Wilson et al., 2014). Theoretically, N_2 could also be produced from nitrite in particles. Nitrite can only be produced from particle remineralization when some oxygen is available. Thus, as the presence of even trace amounts of oxygen diminishes with depth, more enriched N_2 produced from remineralized nitrite in particles would also decrease. In this case a bacterium using remineralized nitrite in a particle would start with a reactant at ~4‰. As the proportion of N_2 produced with this remineralized nitrite decreased with depth, utilization of depleted water column nitrite would become dominant. For example, a simple calculation using St 161 as a template (Fig S2), assuming water column nitrite of -16‰, and N_2 excess of -12‰ at the top of the ODZ with a constant nitrite reduction isotope of effect of 10‰, approximately 70% of nitrite reduced would need to be from particles (producing N_2 at -6‰) and ~30% from the water column (producing N_2 at -26‰). While at 300m, the measured N_2 excess (-25‰) could be reproduced by using 100% water column nitrite. This hypothesis could explain the apparent change in isotope effect with depth along with changes in $\Delta^{15}N_{NO2\text{-}N2}$ values. Additionally, the large use of remineralized organic matter in this scenario would also be consistent with our calculated 5.3‰ $DIN_{initial}$ values, which reflect remineralization.

While nitrite oxidation, migrating zooplankton and mixing between water masses undoubtedly occur in the ODZ and may affect our isotope values, alone they cannot explain our variability in isotope effects. However, both a shift between denitrifiers with and without an internal nitrite pool or denitrification inside sinking particles can explain our ETNP data.

4.4 Magnitude of N_2 production isotope effect

Lately, evidence has mounted for a small fractionation effect (<15‰) for water column denitrification. This small fractionation effect is based on culture experiments and isotopic data from the ETSP (Bourbonnais et al., 2015; Casciotti et al., 2013; Hu et al., 2016; Kritee et al., 2012). However, our data from the heart of the ETNP indicates a large apparent isotope effect of 26±11‰, calculated from DIN, or 27±6‰, calculated from N_2 excess. Similarly our data from the Arabian Sea also indicated a large apparent closed isotope effect of 26±4‰ from $\delta^{15}N$-N_2 excess and 26±3‰ for $\delta^{15}N$-DIN. Our result also contrasts with isotope effect calculations derived from DIN data collected on in the ETSP ODZ, which ranged from 11‰ to 14‰ (Bourbonnais et al., 2015; Hu et al., 2016). Additionally, nitrate reduction and DIN isotope effects are similar in the ETNP and Arabian Sea, but have been repeatedly found to differ in the ETSP (Bourbonnais et al., 2015; Casciotti et al., 2013; Peters et al. this issue). The isotope effect calculation is extremely sensitive to the fraction remaining, which often depends on phosphate in N deficit calculations, but Hu et al (2016), Bourbonnais et al (2015), and our calculations avoid this issue by using measured N_2 excess instead of N deficit in the fraction remaining calculations. The difference between our isotope effects and published isotope effects from the ETSP could be due to differences associated with the location of sampling in those studies. One of the ETSP studies was coastal with bottom depths less than 150m (Hu et al., 2016) and the other two were from eddies influenced by coastal water (Altabet et al., 2012; Bourbonnais et al., 2015). Nitrate concentrations were greatly reduced on these study sites compared to our stations (Altabet et al., 2012; Bourbonnais et al., 2015; Hu et al., 2016). On the coastal transect, there were mismatches between N_2 excess and N deficit (Hu et al., 2016). Data from an along shore transect in the ETSP in 2013 also found mismatches between N_2 excess and N deficit at some stations (Peters et al., this issue). The coastal ETSP shelf, where $\delta^{15}N$-N_2 excess was examined, was affected by sediments (Hu et al., 2016), which have near zero isotope effects (Brandes and Devol, 1997; Lehmann et al., 2007). Perhaps, due to the larger width of the Peru shelf (Smith and Sandwell, 1997; visualization on http://topex.ucsd.edu/marine_topo), sedimentary processes influence the isotope effects in this region. Our coastal station from the ETNP did not have reduced isotope effects compared to the offshore ETNP (Fig. 7). However, the ETNP shelf in the region sampled was quite narrow (Smith and Sandwell, 1997). It seems that the ETSP system is more complicated in some way than the ETNP and Arabian Sea, which affects the apparent isotope effects calculated there.

Our DIN and N_2 excess isotope effects are apparent isotope effects that include both denitrification and anammox. However, our nitrate reduction isotope effects for the ETNP (-28±6‰), and Arabian Sea (-25±6‰) were also large. In culture, dentirifiers grown at slow rates to mimic the estimated in situ water column rates exhibit small nitrate reduction fractionation effects (Kritee et al., 2012). However, cultures grown at high rates show large fractionation effects (Granger et al., 2008; Kritee et al., 2012). Mounting evidence suggests that denitrifiers are preferentially partitioned onto particles (Ganesh et al., 2015, 2014). In all three ODZs, denitrification rates were high when sinking particles were included (Babbin et al., 2014; Chang et al., 2014). This suggests that much of the denitrification in the ODZ may be taking place at higher growth rates associated with particles and therefore, with a larger fractionation effect.

Implications

The balance between sedimentary denitrification and water column denitrification sets the $\delta^{15}N$ of oceanic nitrate. Assuming that in general sedimentary denitrification has a very small fractionation effect, a small the water-column isotope effect for denitrification allows the calculation of a lower the sedimentary denitrification rate (Altabet, 2007; Brandes and Devol, 2002; DeVries et al., 2012). We find evidence for relatively large isotope effects in all three ODZs implying correspondingly large sedimentary denitrification rates. If the ocean is at steady state, denitrification and N_2 fixation should balance, and have been modeled to do so (DeVries et al., 2013, 2012). However, the balance between denitrification and N_2 fixation also depends on N_2 fixation rates, values for which are presently in a state of flux (Konno et al., 2010; Mohr et al., 2010; Moisander et al., 2010). Older N_2 fixation rates calculated from ^{15}N additions are likely to be underestimates due to problems with the measurement (Konno et al., 2010; Mohr et al., 2010). Additionally, new N_2 fixing organisms with a greater geographic range have been discovered (Moisander et al., 2010), increasing the area for potential N_2 fixation. Correction for these issues may almost double N_2 fixation rates (Großkopf et al., 2012). Due to the current uncertainty in N_2 fixation estimates, even the large fractionation effects calculated here do not preclude a balanced N budget (DeVries et al., 2012).

Acknowledgements

We thank Matthew Forbes for technical assistance with the nitrate and nitrite isotope analyses. We thank Steve Emerson and Paul Quay for use of their lab space and facilities, and to Johnny Stutsman, Mark Haught, and Chuck Stump for assistance during the N_2 gas measurement process. Thank you to the captain and crew of the R/V Thompson, and to co-Chief Scientist B.B. Ward. We thank Rick Keil for $\delta^{15}N$ of sediment trap material, and Aaron Morello for shipboard nutrient analyses. Thanks to Justin Penn for discussions.
This work was supported by the US National Science Foundation OCE 1029316 and OCE-0647981 to AHD and OCE 1140404 to KLC. BXC was partially funded by the Joint Institute for the Study of the Atmosphere and Ocean (JISAO) under NOAA Cooperative Agreement NA10OAR4320148 (2010-2015) and NA15OAR4320063 (2015-2020), Contribution No. 2017-072. This is NOAA-PMEL contribution no. 4633.

Funding: This work was supported by the National Science Foundation [grant numbers: OCE-1029316, OCE-0647981 and OCE 1140404].

References

Altabet, M.A., 2007. Constraints on oceanic N balance / imbalance from sedimentary 15N records. Biogeosciences 4, 75–86.

Altabet, M. a., 2001. Nitrogen isotopic evidence for micronutrient control of fractional NO3- utilization in the equatorial Pacific. Limnol. Oceanogr. 46, 368–380. doi:10.4319/lo.2001.46.2.0368

Altabet, M. a., Ryabenko, E., Stramma, L., Wallace, D.W.R., Frank, M., Grasse, P., Lavik, G., 2012. An eddy-stimulated hotspot for fixed nitrogen-loss from the Peru oxygen minimum zone. Biogeosciences 9, 4897–4908. doi:10.5194/bg-9-4897-2012

Babbin, A.R., Bianchi, D., Jayakumar, A., Ward, B.B., 2015. Rapid nitrous oxide cycling in the suboxic ocean. Science (80-.). 348, 1127–1129. doi:10.1126/science.aaa8380

Babbin, A.R., Keil, R.G., Devol, A.H., Ward, B.B., 2014. Oxygen Control Nitrogen Loss in the Ocean. Science (80-.). 344, 406.

Babbin, A.R., Peters, B.D., Mordy, C.W., Widner, B., Casciotti, K.L., Ward, B.B., 2017. Novel metabolisms support the anaerobic nitrite budget in the Eastern Tropical South Pacific. Global Biogeochem. Cycles 31, 258–271. doi:10.1002/2016GB005407

Bianchi, D., Babbin, a. R., Galbraith, E.D., 2014. Enhancement of anammox by the excretion of diel vertical migrators. Proc. Natl. Acad. Sci. 111, 15653–15658. doi:10.1073/pnas.1410790111

Bohlke, J.K., Mroczkowski, S.K., Coplen, T.B., 2003. Oxygen isotopes in nitrate: new reference materials for O-18: O-17: O-16 measurements and observations on nitrate-water equlibration. Rapid Commun. Mass Spectrom. 17, 1835–1846.

Bourbonnais, A., Altabet, M.A., Charoenpong, C.N., Larkum, J., Hu, H., Bange, H.W., Stramma, L., 2015. N-loss isotope effects in Peru oxygen minimum zone studied using a mesoscale eddy as a natural tracer experiment. Global Biogeochem. Cycles 29, 793–811. doi:10.1002/2014GB005001.Received

Brandes, J.A., Devol, A.H., 2002. A global marine-fixed nitrogen isotopic budget : Implications for Holocene nitrogen cycling. Global Biogeochem. Cycles 16, 1120. doi:10.1029/2001GB001856

Brandes, J.A., Devol, A.H., 1997. Isotope fractionation of oxygen and nitrogen in coastal marine sediments. Geochim. Cosmochim. Acta 61, 1793–1801.

Brandes, J.A., Rd, B.B., Devol, H., 1998. Isotopic composition of nitrate in the central Arabian Sea and eastern North Pacific : A tracer for mixing and nitrogen cycles. Limnol. Oceanogr. 43, 1680–1689.

Bristow, L.A., Dalsgaard, T., Tiano, L., Mills, D.B., Bertagnolli, A.D., Wright, J.J., Hallam, S.J., Ulloa, O., Canfield, D.E., Peter, N., Thamdrup, B., 2016. Ammonium and nitrite oxidation at nanomolar oxygen concentrations in oxygen minimum zone waters. Proc. Natl. Acad. Sci. 113, 10601–6. doi:10.1073/pnas.1600359113

Brunner, B., Contreras, S., Lehmann, M.F., Matantseva, O., Rollog, M., Kalvelage, T., Klockgether, G., Lavik, G., Jetten, M.S.M., Kartal, B., Kuypers, M.M.M., 2013. Nitrogen isotope effects induced by anammox bacteria. Proc. Natl. Acad. Sci. 110, 18994–9. doi:10.1073/pnas.1310488110

Buchwald, C., Casciotti, K.L., 2010. Oxygen isotopic fractionation and exchange during bacterial nitrite oxidation. Limnol. Oceanogr. 55, 1064–1074.

Buchwald, C., Santoro, A.E., Stanley, R.H.R., Casciotti, K.L., 2015. Nitrogen cycling in the secondary nitrite maximum of the eastern tropical North Pacific off Costa Rica. Global Biogeochem. Cycles 29, 2061–2081. doi:10.1002/2015GB005187

Casciotti, K., Bohlke, J., McIlvin, M., Mroczkowski, SJ Hannon, J., 2007. Oxygen isotopes in nitrite: Analysis, calibration, and equilibration. Anal. Chem. 79, 2427–2436.

Casciotti, K.L., 2009. Inverse kinetic isotope fractionation during bacterial nitrite oxidation.

688 Geochim. Cosmochim. Acta 73, 2061–2076. doi:10.1016/j.gca.2008.12.022
689 Casciotti, K.L., Buchwald, C., Mcilvin, M., 2013. Deep-Sea Research I Implications of nitrate
690 and nitrite isotopic measurements for the mechanisms of nitrogen cycling in the Peru
691 oxygen de fi cient zone. Deep. Res. Part I 80, 78–93. doi:10.1016/j.dsr.2013.05.017
692 Casciotti, K.L., McIlvin, M.R., 2007. Isotopic analyses of nitrate and nitrite from reference
693 mixtures and application to Eastern Tropical North Pacific waters. Mar. Chem. 107, 184–
694 201. doi:10.1016/j.marchem.2007.06.021
695 Casciotti, K.L., Sigman, D.M., Hastings, M.G., Bohlke, J.K., Hilkert, a, 2002. Measurement of
696 the oxygen isotopic composition of nitrate seawater and freshwater using the dentirifier
697 method. Anal. Chem. 74, 4905–4912. doi:10.1021/ac020113w
698 Chang, B.X., Devol, A.H., Emerson, S.R., 2012. Fixed nitrogen loss from the eastern tropical
699 North Pacific and Arabian Sea oxygen deficient zones determined from measurements of N
700 2 :Ar. Global Biogeochem. Cycles 26, GB004207. doi:10.1029/2011GB004207
701 Chang, B.X., Devol, A.H., Emerson, S.R., 2010. Denitrification and the nitrogen gas excess in
702 the eastern tropical South Pacific oxygen deficient zone. Deep Sea Res. Part I Oceanogr.
703 Res. Pap. 57, 1092–1101. doi:10.1016/j.dsr.2010.05.009
704 Chang, B.X., Rich, J.R., Jayakumar, A., Naik, H., Pratihary, A.K., Keil, R.G., Ward, B.B.,
705 Devol, A.H., 2014. The effect of organic carbon on fixed nitrogen loss in the eastern
706 tropical South Pacific and Arabian Sea oxygen deficient zones. Limnol. Oceanogr. 59,
707 1267–1274. doi:10.4319/lo.2014.59.4.1267
708 Chronopoulou, P.-M., Shelley, F., Pritchard, W.J., Maanoja, S.T., Trimmer, M., 2017. Origin
709 and fate of methane in the Eastern Tropical North Pacific oxygen minimum zone. ISME J.
710 11, 1386–1399. doi:10.1038/ismej.2017.6
711 Cline, J.D., Kaplan, I.R., 1975. ISOTOPIC FRACTIONATION OF DISSOLVED NITRATE
712 DURING DENI- TRIFICATION IN THE EASTERN TROPICAL NORTH PACIFIC
713 OCEAN. Mar. Chem. 3, 271–299.
714 Dähnke, K., Thamdrup, B., 2013. Nitrogen isotope dynamics and fractionation during
715 sedimentary denitrification in Boknis Eck, Baltic Sea. Biogeosciences 10, 3079–3088.
716 doi:10.5194/bg-10-3079-2013
717 De Brabandere, L., Canfield, D.E., Dalsgaard, T., Friederich, G.E., Revsbech, N.P., Ulloa, O.,
718 Thamdrup, B., 2014. Vertical partitioning of nitrogen-loss processes across the oxic-anoxic

719 interface of an oceanic oxygen minimum zone. Environ. Microbiol. 16, 3041–3054.
720 doi:10.1111/1462-2920.12255
721 Deutsch, C., Brix, H., Ito, T., Frenzel, H., Thompson, L., 2011. Climate-forced variability of
722 ocean hypoxia. Science 333, 336–339. doi:10.1126/science.1202422
723 DeVries, T., Deutsch, C., Primeau, F., Chang, B., Devol, A., 2012. Global rates of water-column
724 denitrification derived from nitrogen gas measurements. Nat. Geosci. 5, 547–550.
725 doi:10.1038/ngeo1515
726 DeVries, T., Deutsch, C., Rafter, P. a., Primeau, F., 2013. Marine denitrification rates determined
727 from a global 3-D inverse model. Biogeosciences 10, 2481–2496. doi:10.5194/bg-10-2481-
728 2013
729 Emerson, S., Stump, C., Wilbur, D., Quay, P., 1999. Accurate measurement of O2, N2, and Ar
730 gases in water and the solubility of N2. Mar. Chem. 64, 337–347. doi:10.1016/S0304-
731 4203(98)00090-5
732 Fiedler, P.C., Talley, L.D., 2006. Hydrography of the eastern tropical Pacific: A review. Prog.
733 Oceanogr. 69, 143–180. doi:10.1016/j.pocean.2006.03.008
734 Fuchsman, C.A., Devol, A.H., Saunders, J.K., McKay, C., Rocap, G., 2017. Niche Partitioning
735 of the N cycling microbial community of an offshore Oxygen Deficient Zone. Front.
736 Microbiol. 8, 2384.
737 Fuchsman, C.A., Murray, J.W., Konovalov, S.K., 2008. Concentration and natural stable isotope
738 profiles of nitrogen species in the Black Sea. Mar. Chem. 111, 90–105.
739 doi:10.1016/j.marchem.2008.04.009
740 Ganesh, S., Bristow, L. a, Larsen, M., Sarode, N., Thamdrup, B., Stewart, F.J., 2015. Size-
741 fraction partitioning of community gene transcription and nitrogen metabolism in a marine
742 oxygen minimum zone. ISME J. 9, 2682–2696. doi:10.1038/ismej.2015.44
743 Ganesh, S., Parris, D.J., DeLong, E.F., Stewart, F.J., 2014. Metagenomic analysis of size-
744 fractionated picoplankton in a marine oxygen minimum zone. ISME J. 8, 187–211.
745 doi:10.1038/ismej.2013.144
746 Garcia-Robledo, E., Padilla, C.C., Aldunate, M., Stewart, F.J., Ulloa, O., Paulmier, A., Gregori,
747 G., Revsbech, N.P., 2017. Cryptic oxygen cycling in anoxic marine zones. Proc. Natl. Acad.
748 Sci. 201619844. doi:10.1073/pnas.1619844114
749 Garcia, H.E., Locarnini, R. a, Boyer, T.P., Antonov, J.I., Mishonov, a V, Baranova, O.K.,

750 Zweng, M.M., Reagan, J.R., Johnson, D.R., 2013. World Ocean Atlas 2013. Vol. 3:
751 Dissolved Oxygen, Apparent Oxygen Utilization, and Oxygen Saturation. S. Levitus, Ed.;
752 A. Mishonov, Technical Ed. 3, 27.
753 Gaye, B., Nagel, B., Dähnke, K., Rixen, T., Emeis, K.C., 2013. Evidence of parallel
754 denitrification and nitrite oxidation in the ODZ of the Arabian Sea from paired stable
755 isotopes of nitrate and nitrite. Global Biogeochem. Cycles 27, 1059–1071.
756 doi:10.1002/2011GB004115
757 Granger, J., Sigman, D.M., 2009. Removal of nitrite with sulfamic acid for nitrate N and O
758 isotope analysis with the denitrifier method. Rapid Commun. mass Spectrom. 23, 3753–
759 3762.
760 Granger, J., Sigman, D.M., Lehmann, M.F., Tortell, P.D., 2008. Nitrogen and oxygen isotope
761 fractionation during dissimilatory nitrate reduction by denitrifying bacteria. Limnol.
762 Oceanogr. 53, 2533–2545. doi:10.4319/lo.2008.53.6.2533
763 Granger, J., Vt, C., Sigman, D.M., Needoba, J.A., Harrison, P.J., 2004. Coupled nitrogen and
764 oxygen isotope fractionation of nitrate during assimilation by cultures of marine
765 phytoplankton 49, 1763–1773.
766 Großkopf, T., Mohr, W., Baustian, T., Schunck, H., Gill, D., Kuypers, M.M.M., Lavik, G.,
767 Schmitz, R.A., Wallace, D.W.R., Laroche, J., 2012. Doubling of marine dinitrogen-fixation
768 rates based on direct measurements. Nature 488, 361–364. doi:10.1038/nature11338
769 Hamme, R.C., Emerson, S.R., 2004. The solubility of neon , nitrogen and argon in distilled water
770 and seawater. Deep Sea Res. Part I Oceanogr. Res. Pap. 51, 1517–1528.
771 doi:10.1016/j.dsr.2004.06.009
772 Horak, R.E.A., Ruef, W., Ward, B.B., Devol, A.H., 2016. Expansion of denitrification and
773 anoxia in the eastern tropical North Pacific from 1972 to 2012. Geophys. Res. Lett. 43,
774 5252–5260. doi:10.1002/2016GL068871
775 Hu, H., Bourbonnais, A., Larkum, J., Bange, H.W., Altabet, M.A., 2016. Nitrogen cycling in
776 shallow low-oxygen coastal waters off Peru from nitrite and nitrate nitrogen and oxygen
777 isotopes. Biogeosciences 13, 1453–1468. doi:10.5194/bg-13-1453-2016
778 Ito, T., Deutsch, C., 2013. Variability of the oxygen minimum zone in the tropical North Paci fi c
779 during the late twentieth century. Global Biogeochem. Cycles 27, 1119–1128.
780 doi:10.1002/2013GB004567

781 Ito, T., Deutsch, C., 2006. Understanding the saturation state of argon in the thermocline: The
782 role of air-sea gas exchange and diapycnal mixing. Global Biogeochem. Cycles 20, 1–15.
783 Ito, T., Minobe, S., Long, M.C., Deutsch, C., 2017. Upper ocean O2 trends: 1958–2015.
784 Geophys. Res. Lett. 44, 4214–4223. doi:10.1002/2017GL073613
785 Ito, T., Nenes, A., Johnson, M.S., Meskhidze, N., Deutsch, C., 2016. Acceleration of oxygen
786 decline in the tropical Pacific over the past decades by aerosol pollutants. Nat. Geosci. 9,
787 443–448. doi:10.1038/NGEO2717
788 Jayakumar, A., Chang, B.X., Widner, B., Bernhardt, P., Mulholland, M.R., Ward, B.B., 2017.
789 Biological nitrogen fixation in the oxygen-minimum region of the eastern tropical North
790 Pacific ocean. ISME J. online, 1–12. doi:10.1038/ismej.2017.97
791 Jayakumar, D.A., Naqvi, S.W.A., Narvekar, P. V., George, M.D., 2001. Methane in coastal and
792 offshore waters of the Arabian Sea. Mar. Chem. 74, 1–13. doi:10.1016/S0304-
793 4203(00)00089-X
794 Jensen, M.M., Petersen, J., Dalsgaard, T., Thamdrup, B., 2009. Pathways, rates, and regulation
795 of N2 production in the chemocline of an anoxic basin, Mariager Fjord, Denmark. Mar.
796 Chem. 113, 102–113. doi:10.1016/j.marchem.2009.01.002
797 Keil, R.G., Neibauer, J.A., Biladeau, C., Van Der Elst, K., Devol, A.H., 2016. A multiproxy
798 approach to understanding the “enhanced” flux of organic matter through the oxygen-
799 deficient waters of the Arabian Sea. Biogeosciences 13, 2077–2092. doi:10.5194/bg-13-
800 2077-2016
801 Knox, M., Quay, P.D., Wilbur, D.O., 1992. Kinetic isotopic fractionation during air□water gas
802 transfer of O2, N2, CH4, and H2. J. Geophys. Res. … 97, 335–343. doi:10.1029/92JC00949
803 Konno, U., Tsunogai, U., Komatsu, D.D., Daita, S., Nakagawa, F., Tsuda, A., Matsui, T., Eum,
804 Y.-J., Suzuki, K., 2010. Determination of total N 2 fixation rates in the ocean taking into
805 account both the particulate and filtrate fractions. Biogeosciences 7, 2369–2377.
806 doi:10.5194/bg-7-2369-2010
807 Kritee, K., Sigman, D.M., Granger, J., Ward, B.B., Jayakumar, A., Deutsch, C., 2012. Reduced
808 isotope fractionation by denitrification under conditions relevant to the ocean. Geochim.
809 Cosmochim. Acta 92, 243–259. doi:10.1016/j.gca.2012.05.020
810 Lehmann, M.F., Sigman, D.M., Mccorkle, D.C., Granger, J., Hoffmann, S., Cane, G., Brunelle,
811 B.G., 2007. The distribution of nitrate 15 N / 14 N in marine sediments and the impact of

benthic nitrogen loss on the isotopic composition of oceanic nitrate. Geochim. Cosmochim. Acta 71, 5384–5404. doi:10.1016/j.gca.2007.07.025

Macko, S.A., Engel, M.H., Qian, Y., 1994. Early diagenesis and organic matter preservation - a molecular stable carbon isotope perspective. Chem. Geol. 114, 365–379. doi:10.1016/0009-2541(94)90064-7

Manning, C.C., Hamme, R.C., Bourbonnais, A., 2010. Impact of deep-water renewal events on fi xed nitrogen loss from seasonally-anoxic Saanich Inlet. Mar. Chem. 122, 1–10. doi:10.1016/j.marchem.2010.08.002

Marconi, D., Kopf, S., Rafter, P.A., Sigman, D.M., 2017. Aerobic respiration along isopycnals leads to overestimation of the isotope effect of denitrification in the ocean water column. Geochim. Cosmochim. Acta 197, 417–432. doi:10.1016/j.gca.2016.10.012

Mariotti, A., Germon, J.C., Hubert, P., Kaiser, P., Letolle, R., Tardieux, A., Tardieux, P., 1981. Experimental determination of nitrogen kinetic isotope fractionation-some principles--Illustration for the denitrification and nitrification processes. Plant Soil 62, 413–430.

Martin, T.S., Casciotti, K.L., 2017. Paired N and O isotopic analysis of nitrate and nitrite in the Arabian Sea oxygen deficient zone. Deep. Res. Part I Oceanogr. Res. Pap. 121, 121–131. doi:10.1016/j.dsr.2017.01.002

Martin, T.S., Casciotti, K.L., 2016. Nitrogen and oxygen isotopic fractionation during microbial nitrite reduction. Limnol. Oceanogr. 61, 1134–1143. doi:10.1002/lno.10278

McIlvin, M.R., Altabet, M.A., 2005. Chemical conversion of nitrate and nitrite to nitrous oxide for nitrogen and oxygen isotopic analysis in freshwater and seawater. Anal Chem 77, 5589–5595. doi:10.1021/ac050528s

McIlvin, M.R., Casciotti, K.L., 2011. Technical Updates to Bacterial method for nitrate isotopic analyses. Anal. Chem. 83, 1850–1856.

Mohr, W., Grosskopf, T., Wallace, D.W.R., LaRoche, J., 2010. Methodological underestimation of oceanic nitrogen fixation rates. PLoS One 5, e12583. doi:10.1371/journal.pone.0012583

Moisander, P.H., Beinart, R.A., Hewson, I., White, A.E., Johnson, K.S., Carlson, C.A., Montoya, J.P., Zehr, J.P., 2010. Unicellular cyanobacterial distributions broaden the oceanic N2 fixation domain. Science (80-.). 327, 1512–4. doi:10.1126/science.1185468

Moore, C.M., Mills, M.M., Arrigo, K.R., Berman-Frank, I., Bopp, L., Boyd, P.W., Galbraith, E.D., Geider, R.J., Guieu, C., Jaccard, S.L., Jickells, T.D., La Roche, J., Lenton, T.M.,

Mahowald, N.M., Marañón, E., Marinov, I., Moore, J.K., Nakatsuka, T., Oschlies, a., Saito, M. a., Thingstad, T.F., Tsuda, a., Ulloa, O., 2013. Processes and patterns of oceanic nutrient limitation. Nat. Geosci. 6, 701–710. doi:10.1038/ngeo1765

Paulmier, A., Ruiz-Pino, D., 2009. Oxygen minimum zones (OMZs) in the modern ocean. Prog. Oceanogr. 80, 113–128. doi:10.1016/j.pocean.2008.08.001

Peng, X., Fuchsman, C.A., Jayakumar, A., Oleynik, S., Martens-habbena, W., 2015. Ammonia and nitrite oxidation in the Eastern Tropical North Pacific. Global Biogeochem. Cycles 29, 2034–2049.

Penn, J., Weber, T., Deutsch, C., 2016. Microbial functional diversity alters the structure and sensitivity of oxygen deficient zones. Geophys. Reserach Lett. 43, 9773–9780. doi:10.1002/2016GL070438

Pennington, J.T., Mahoney, K.L., Kuwahara, V.S., Kolber, D.D., Calienes, R., Chavez, F.P., 2006. Primary production in the eastern tropical Pacific: A review. Prog. Oceanogr. 69, 285–317. doi:10.1016/j.pocean.2006.03.012

Peters, B.D., Babbin, A.R., Lettmann, K.A., Mordy, C.W., Ulloa, O., Ward, B.B., Casciotti, K.L., 2016. Vertical modeling of the nitrogen cycle in the eastern tropical South Pacific oxygen deficient zone using high-resolution concentration and isotope measurements. Global Biogeochem. Cycles 30, GB005415. doi:10.1002/2016GB005415.Received

Rafter, P.A., Difiore, P.J., Sigman, D.M., 2013. Coupled nitrate nitrogen and oxygen isotopes and organic matter remineralization in the Southern and Pacific Oceans. J. Geophys. Res. Ocean. 118, 4781–4794. doi:10.1002/jgrc.20316

Reeburgh, W.S., Ward, B.B., Whalen, S.C., Sandbeck, K.A., Kilpatrickt, K.A., Kerkhof, L.J., 1991. Black Sea methane geochemistry. Deep Sea Res. Part A. Oceanogr. Res. Pap. 38, S1189–S1210. doi:10.1016/S0198-0149(10)80030-5

Revsbech, N.P., Larsen, L.H., Gundersen, J., Dalsgaard, T., Ulloa, O., Thamdrup, B., 2009. Determination of ultra-low oxygen concentrations in oxygen minimum zones by the STOX sensor. Limnol. Oceanogr. 7, 371–381.

Saino, T., Hattori, A., 1980. 15N natural abundance in oceanic suspended particulate matter. Nature 283, 752–754. doi:10.1038/283752a0

Sigman, D.M., Casciotti, K.L., Andreani, M., Barford, C., Galanter, M., Böhlke, J.K., 2001. A bacterial method for the nitrogen isotopic analysis of nitrate in seawater and freshwater.

874 Anal. Chem. 73, 4145–4153. doi:10.1021/ac010088e
875 Sigman, D.M., Difiore, P.J., Hain, M.P., Deutsch, C., Karl, D.M., Bo, V., 2009. Sinking organic
876 matter spreads the nitrogen isotope signal of pelagic denitrification in the North Pacific.
877 Geophys. Res. Lett. 36, 1–5. doi:10.1029/2008GL035784
878 Sigman, D.M., Robinson, R., Knapp, A.N., Geen, A. Van, Mccorkle, D.C., Brandes, J.A.,
879 Thunell, R.C., 2003. Distinguishing between water column and sedimentary denitrification
880 in the Santa Barbara Basin using the stable isotopes of nitrate. Geochemistry Geophys.
881 Geosystems 4, 1040. doi:10.1029/2002GC000384
882 Smith, W.H., Sandwell, D., 1997. Global Sea Floor Topography from Satellite Altimetry and
883 Ship Depth Soundings. Science (80-.). 277, 1956–1962.
884 doi:10.1126/science.277.5334.1956
885 Stramma, L., Johnson, G.C., Sprintall, J., Mohrholz, V., 2008. Expanding Oxygen-Minimum
886 Zones in the Tropical Oceans. Science (80-.). 320, 655–658.
887 Ulloa, O., Delong, E.F., Letelier, R.M., Stewart, F.J., 2012. Microbial oceanography of anoxic
888 oxygen minimum zones. Proc. Natl. Acad. Sci. 109, 15996–16003.
889 doi:10.1073/pnas.1205009109
890 UNESCO, 1994. Protocols for the Joint Global Ocean Flux Study (JGOFS) Core Measurements.
891 New York.
892 Voss, M., Dippner, J.W., Montoya, J.P., 2001. Nitrogen isotope patterns in the oxygen-de “ cient
893 waters of the Eastern Tropical North Paci ” c Ocean. Deep Sea Res. Part I Oceanogr. Res.
894 Pap. 48, 1905–1921.
895 Wada, E., 1980. Nitrogen isotope fractionation in biogeochemical processes occuring in marine
896 environments., in: Goldberg, E.D., Horibe, Y. (Eds.), Isotope Marine Chemistry. Uchida
897 Rokakuho, Tokyo, pp. 375–398.
898 Ward, B.B., Devol, A.H., Rich, J.J., Chang, B.X., Bulow, S.E., Naik, H., Pratihary, A.K.,
899 Jayakumar, A., 2009. Denitrification as the dominant nitrogen loss process in the Arabian
900 Sea. Nature 461, 78.
901 Whitney, F.A., Freeland, H.J., Robert, M., 2007. Persistently declining oxygen levels in the
902 interior waters of the eastern subarctic Pacific. Prog. Oceanogr. 75, 179–199.
903 doi:10.1016/j.pocean.2007.08.007
904 Wilson, S.T., del Valle, D.A., Segura-Noguera, M., Karl, D.M., 2014. A role for nitrite in the

production of nitrous oxide in the lower euphotic zone of the oligotrophic North Pacific Ocean. Deep. Res. Part I Oceanogr. Res. Pap. 85, 47–55. doi:10.1016/j.dsr.2013.11.008

Figure Captions:

Figure 1. Schematic depicting individual isotope effects and N sources that are included in the apparent isotope effect for N_2 production.

Figure 2. A map of the Eastern Tropical North Pacific shaded by oxygen concentration according to the World Ocean Atlas (2013) (Garcia et al., 2013) at density surface σ=26.5. Black dots indicate stations examined in this paper.

Figure 3. Section plot of A) oxygen (μmol/kg), B) nitrite (μmol/kg) and C) potential density (kg/m^3) for the ETNP in 2012. Sampled depths are indicated by black dots. Station names are listed at the top of part A and include some stations where isotope data was not available. The shelf is indicated by dark grey.

Figure 4. Compilation of ETNP N concentrations (A) and isotopes (B) for offshore stations (St 135-164) plotted versus depth. Dashed lines indicate the boundaries of the ODZ using STOX oxygen electrode measurements from Tiano et al. (2014).

Figure 5. $\delta^{15}N$ data for the Arabian Sea St 1. The $\delta^{15}N$ of N_2 excess is calculated by subtracting background values. Red triangles are $\delta^{15}N$ of N_2 excess for a background value of 0.68‰ (Knox et al., 1992). Red lines indicate the range of values if background is varied between 0.65‰ and 0.7‰. $\delta^{15}N$-NO_2- is also shown where available (green circles). Nitrite concentrations (lower axis) are shown for comparison (blue triangles). Dashed lines indicate the boundaries of the ODZ.

Figure 6. A compilation of $\Delta^{15}N$ for the difference between nitrate and nitrite and for the difference between N_2 and nitrite for the secondary nitrite peak at both offshore and coastal stations in the ETNP. All data points are in the ODZ.

Figure 7. Variability of the isotope effect (ε) for N_2 production ($\delta^{15}N$-DIN or $\delta^{15}N$-N_2 excess) with depth in the ETNP at A) an average of offshore stations 135-164 (individual stations can be seen in Figure S12) and B) at coastal station 132 (bottom depth 550m). Red lines indicate what the fractionation factor would be if the background was shifted from 0.68‰ (Knox et al., 1992) to either 0.65‰ or 0.7‰.

Figure 8. Closed system fractionation factors for the Arabian Sea in 2007. Red lines indicate what the fractionation factor would be if the background was shifted from 0.68‰ (Knox et al., 1992) to either 0.65‰ or 0.7‰.

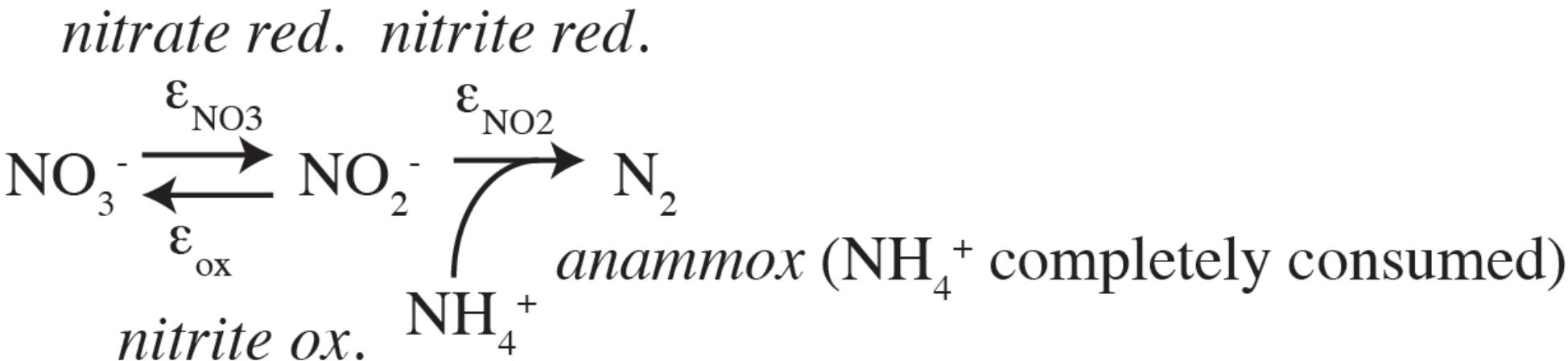
nitrate red.
nitrite red.
ε_{NO3}
ε_{NO2}
NO_3^-
NO_2^-
N_2
ε_{ox}
anammox (NH_4^+ completely consumed)
nitrite ox.
NH_4^+

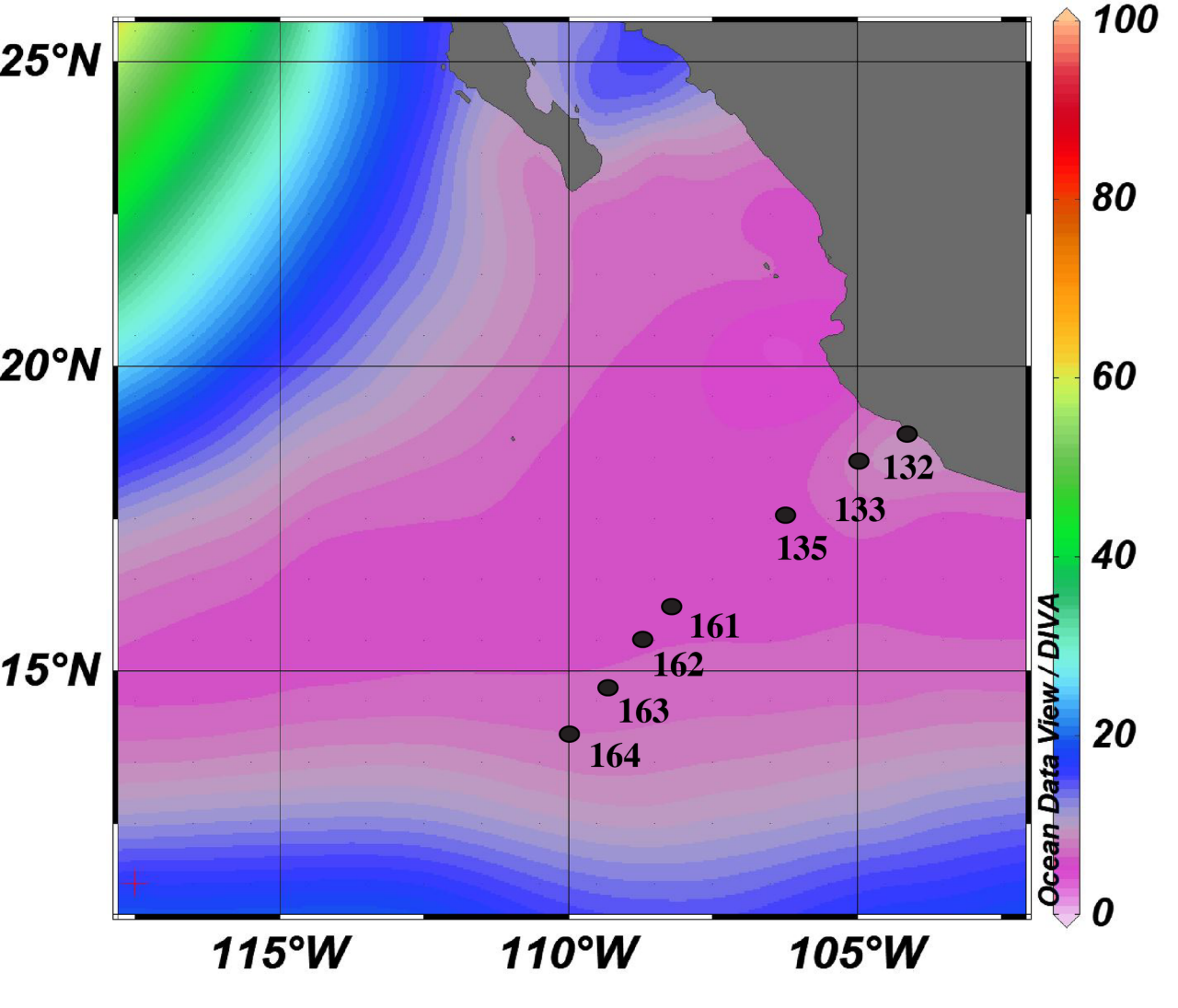
25°N
20°N
15°N
115°W
110°W
105°W
132
133
135
161
162
163
164
100
80
60
40
20
0
Ocean Data View / DIVA

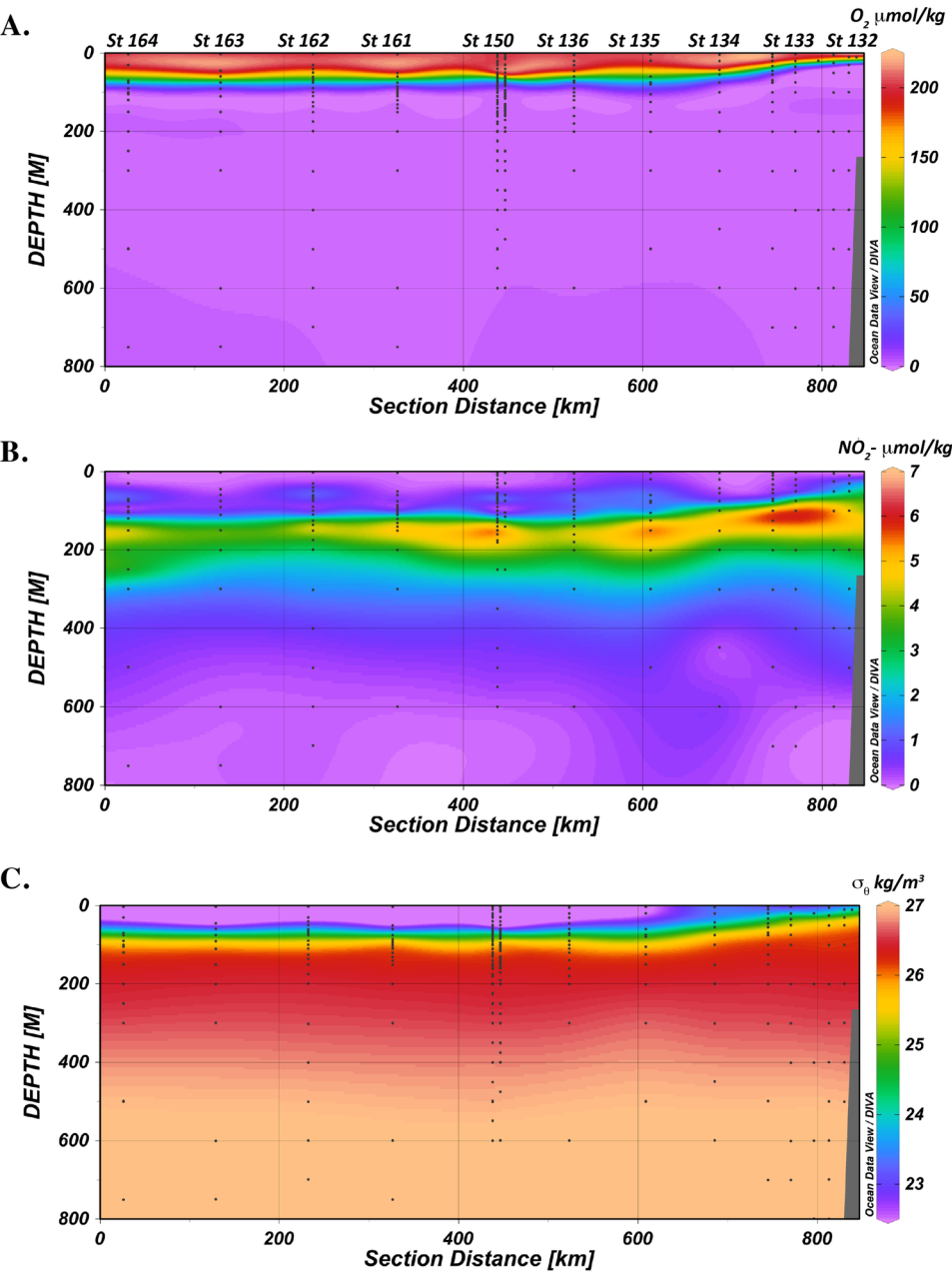
A.
St 164
St 163
St 162
St 161
St 150
St 136
St 135
St 134
St 133
St 132
O_2 µmol/kg
200
150
100
50
0
DEPTH [M]
0
200
400
600
800
Section Distance [km]
Ocean Data View / DIVA
B.
NO_2^- µmol/kg
7
6
5
4
3
2
1
0
C.
σ_0 kg/m³
27
26
25
24
23

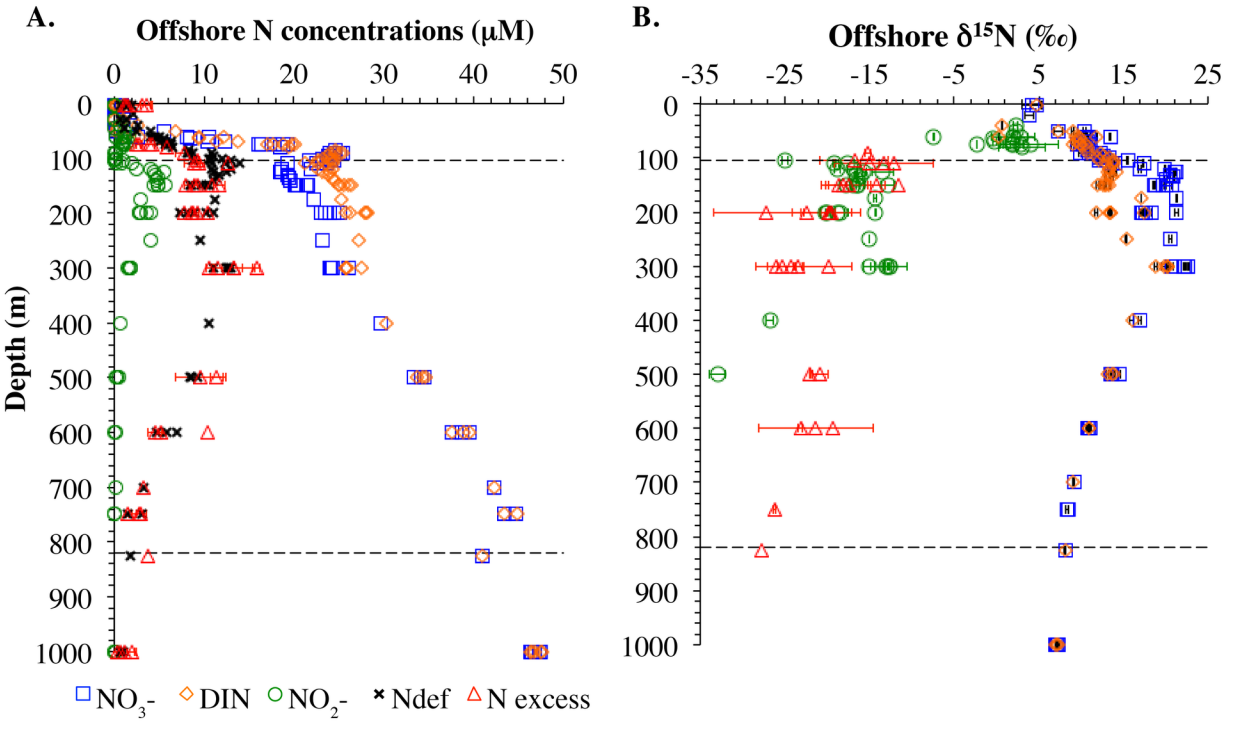
A.
Offshore N concentrations (μM)
0
10
20
30
40
50
Depth (m)
0
100
200
300
400
500
600
700
800
900
1000
NO3-
DIN
NO2-
Ndef
N excess
B.
Offshore δ15N (‰)
-35
-25
-15
-5
5
15
25

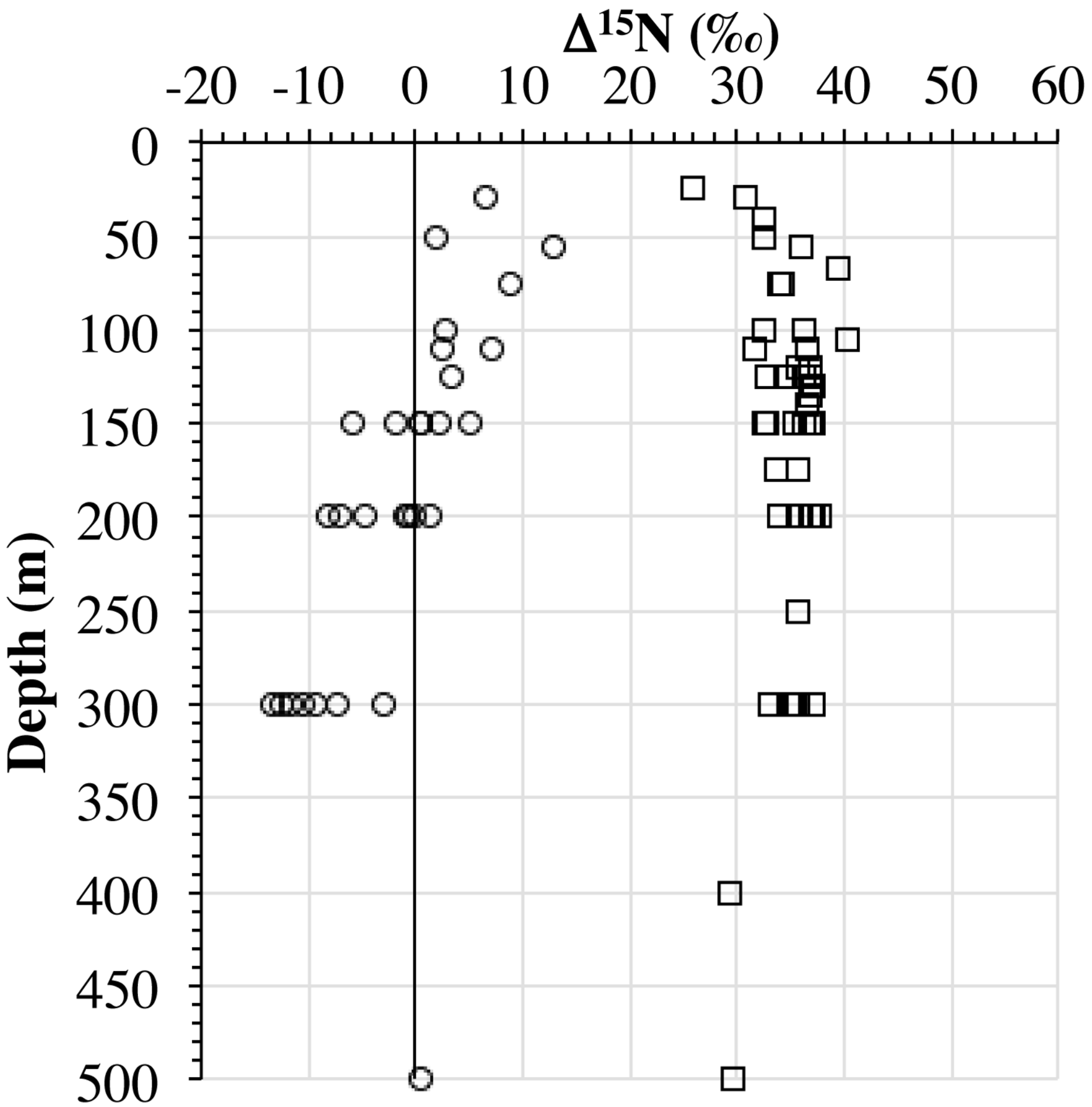
Δ15N (‰)
-20
-10
0
10
20
30
40
50
60
Depth (m)
0
50
100
150
200
250
300
350
400
450
500

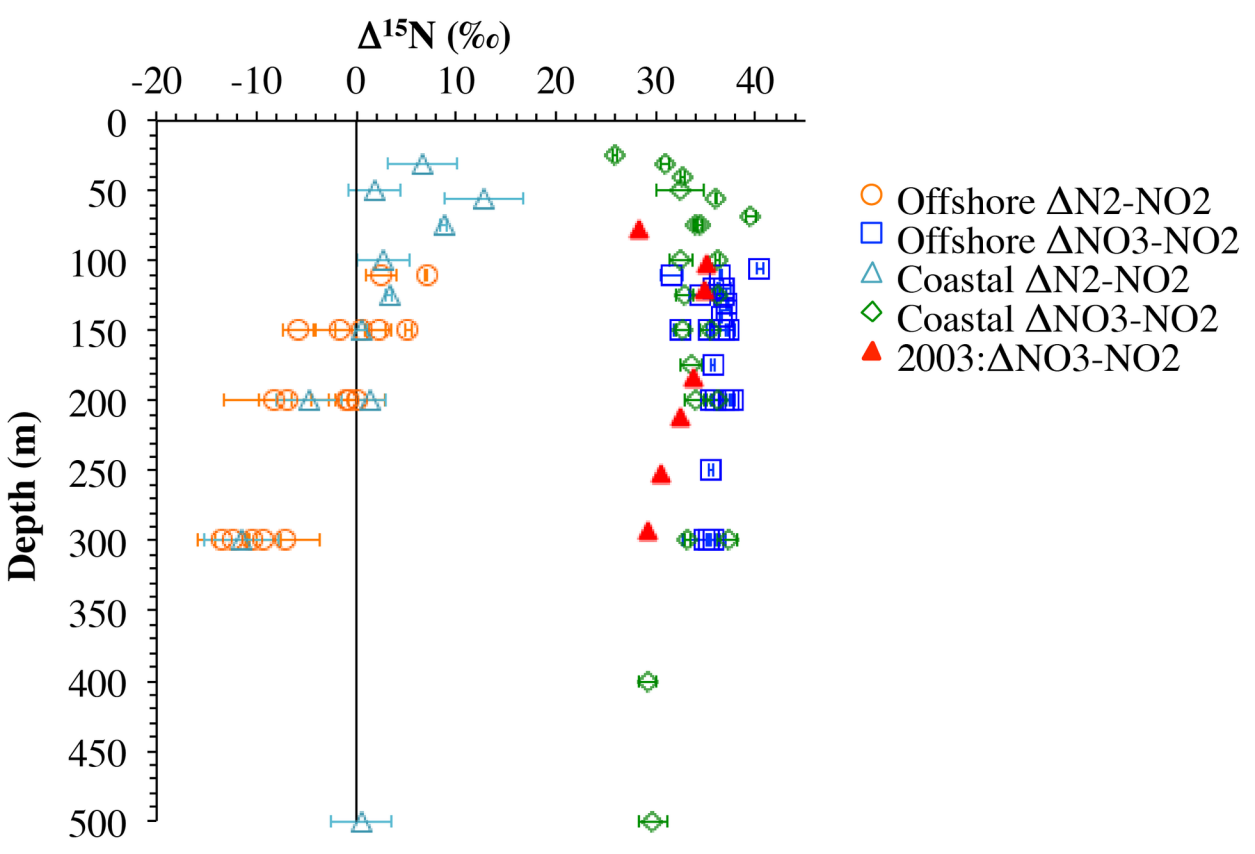
Δ15N (‰)
-20
-10
0
10
20
30
40
Depth (m)
0
50
100
150
200
250
300
350
400
450
500
Offshore ΔN2-NO2
Offshore ΔNO3-NO2
Coastal ΔN2-NO2
Coastal ΔNO3-NO2
2003:ΔNO3-NO2

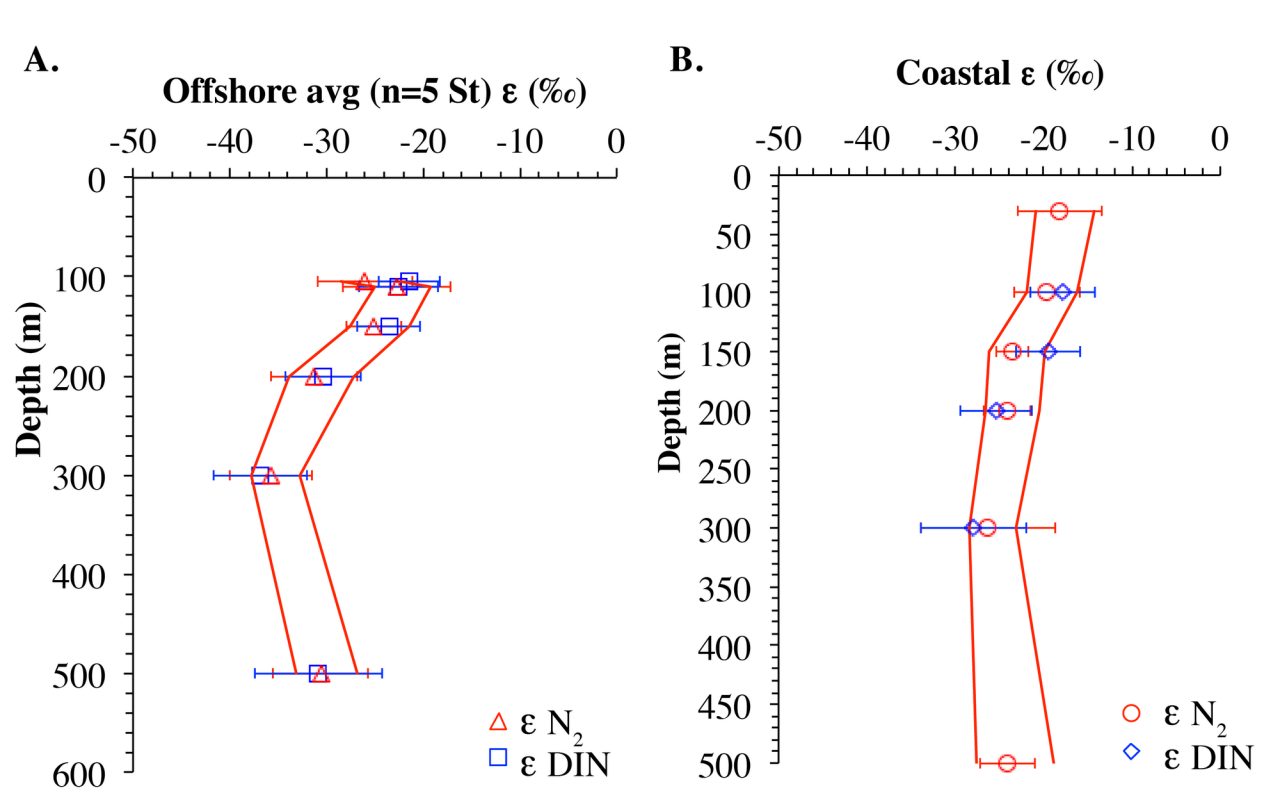
A.
Offshore avg (n=5 St) ε (‰)
-50
-40
-30
-20
-10
0
Depth (m)
0
100
200
300
400
500
600
ε N2
ε DIN
B.
Coastal ε (‰)
-50
-40
-30
-20
-10
0
Depth (m)
0
50
100
150
200
250
300
350
400
450
500
ε N2
ε DIN

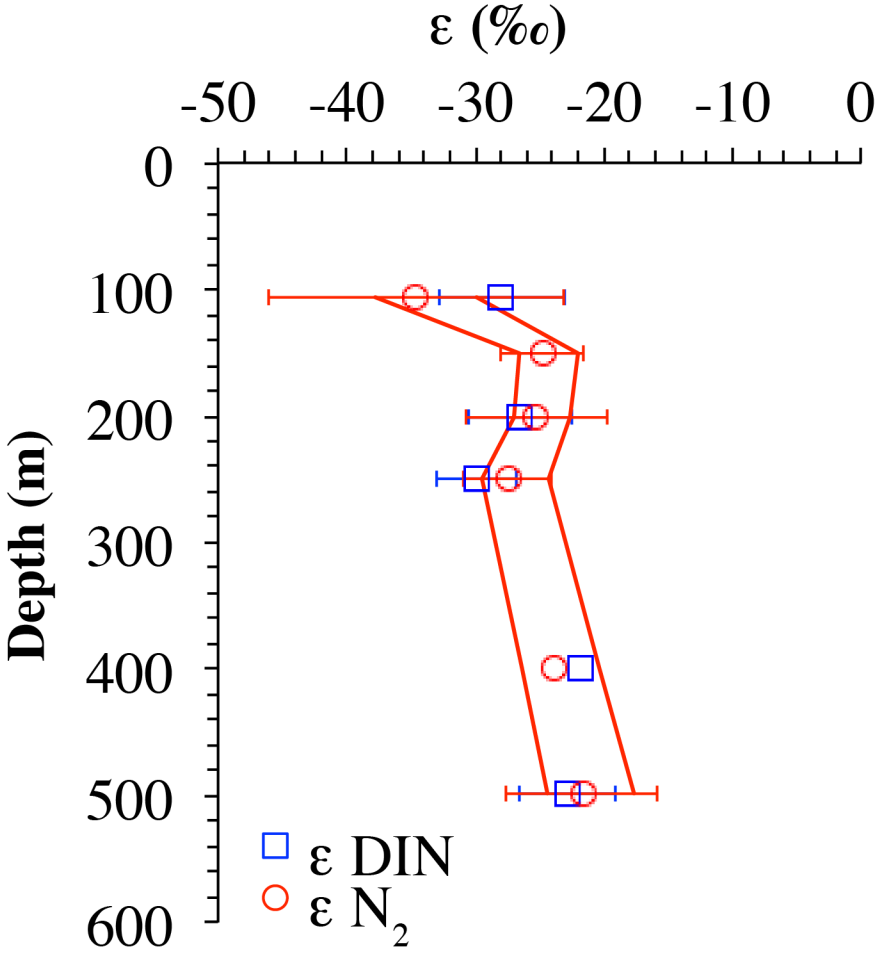
ε (‰)
-50
-40
-30
-20
-10
0
Depth (m)
0
100
200
300
400
500
600
ε DIN
ε N2